

SARS-CoV-2-specific T cell therapy for severe COVID-19: a randomized phase 1/2 trial

Received: 4 November 2022

Accepted: 28 June 2023

Published online: 17 July 2023

 Check for updates

A list of authors and their affiliations appears at the end of the paper

Despite advances, few therapeutics have shown efficacy in severe coronavirus disease 2019 (COVID-19). In a different context, virus-specific T cells have proven safe and effective. We conducted a randomized (2:1), open-label, phase 1/2 trial to evaluate the safety and efficacy of off-the-shelf, partially human leukocyte antigen (HLA)-matched, convalescent donor-derived severe acute respiratory syndrome coronavirus 2 (SARS-CoV-2)-specific T cells (CoV-2-STs) in combination with standard of care (SoC) in patients with severe COVID-19 compared to SoC during Delta variant predominance. After a dose-escalated phase 1 safety study, 90 participants were randomized to receive CoV-2-ST+SoC ($n = 60$) or SoC only ($n = 30$). The co-primary objectives of the study were the composite of time to recovery and 30-d recovery rate and the *in vivo* expansion of CoV-2-STs in patients receiving CoV-2-ST+SoC over SoC. The key secondary objective was survival on day 60. CoV-2-ST+SoC treatment was safe and well tolerated. The study met the primary composite endpoint (CoV-2-ST+SoC versus SoC: recovery rate 65% versus 38%, $P = 0.017$; median recovery time 11 d versus not reached, $P = 0.052$, respectively; rate ratio for recovery 1.71 (95% confidence interval 1.03–2.83, $P = 0.036$)) and the co-primary objective of significant CoV-2-ST expansion compared to SoC (CoV-2-ST+SoC versus SoC, $P = 0.047$). Overall, in hospitalized patients with severe COVID-19, adoptive immunotherapy with CoV-2-STs was feasible and safe. Larger trials are needed to strengthen the preliminary evidence of clinical benefit in severe COVID-19.

Two years after the outbreak of the coronavirus disease 2019 (COVID-19) pandemic, caused by severe acute respiratory syndrome coronavirus 2 (SARS-CoV-2), remarkable joint efforts have been made by the entire scientific community to fight the virus. Vaccines have unequivocally been the most effective advance against the pandemic. In terms of therapeutics, despite the improved outcomes in specific COVID-19 populations with the recently approved molnupiravir and nirmatrelvir/ritonavir (Paxlovid) (for mild to moderate disease at risk for progression)^{1–3} and the interleukin (IL)-6 receptor antagonists (for critical illness under organ support)⁴, hospitalized patients with severe disease lack therapeutic options that provide additional benefit over standard of care (SoC), which includes dexamethasone⁵ and remdesivir⁶.

Antiviral T cells as an alternative therapeutic platform against COVID-19 may hold promise. Specific T cells targeting viruses, including Epstein–Barr virus, adenovirus, cytomegalovirus and BK virus, mainly in the setting of solid organ transplantation or hematopoietic stem cell transplantation (HSCT), have been safely and effectively applied as a prophylaxis or treatment of opportunistic infections^{7–13}. Moreover, we and others have previously shown the key role of T cells in controlling SARS-CoV-2 infection and the feasibility to *ex vivo* expand SARS-CoV-2 memory T cells from convalescent donors^{14–21}.

Here we report the feasibility of generating a bank of SARS-CoV-2-specific T cell (CoV-2-ST) products from convalescent donors, and we assess the safety and efficacy of adoptively transferring

✉ e-mail: apostoloud8@gmail.com; eyannaki@u.washington.edu.

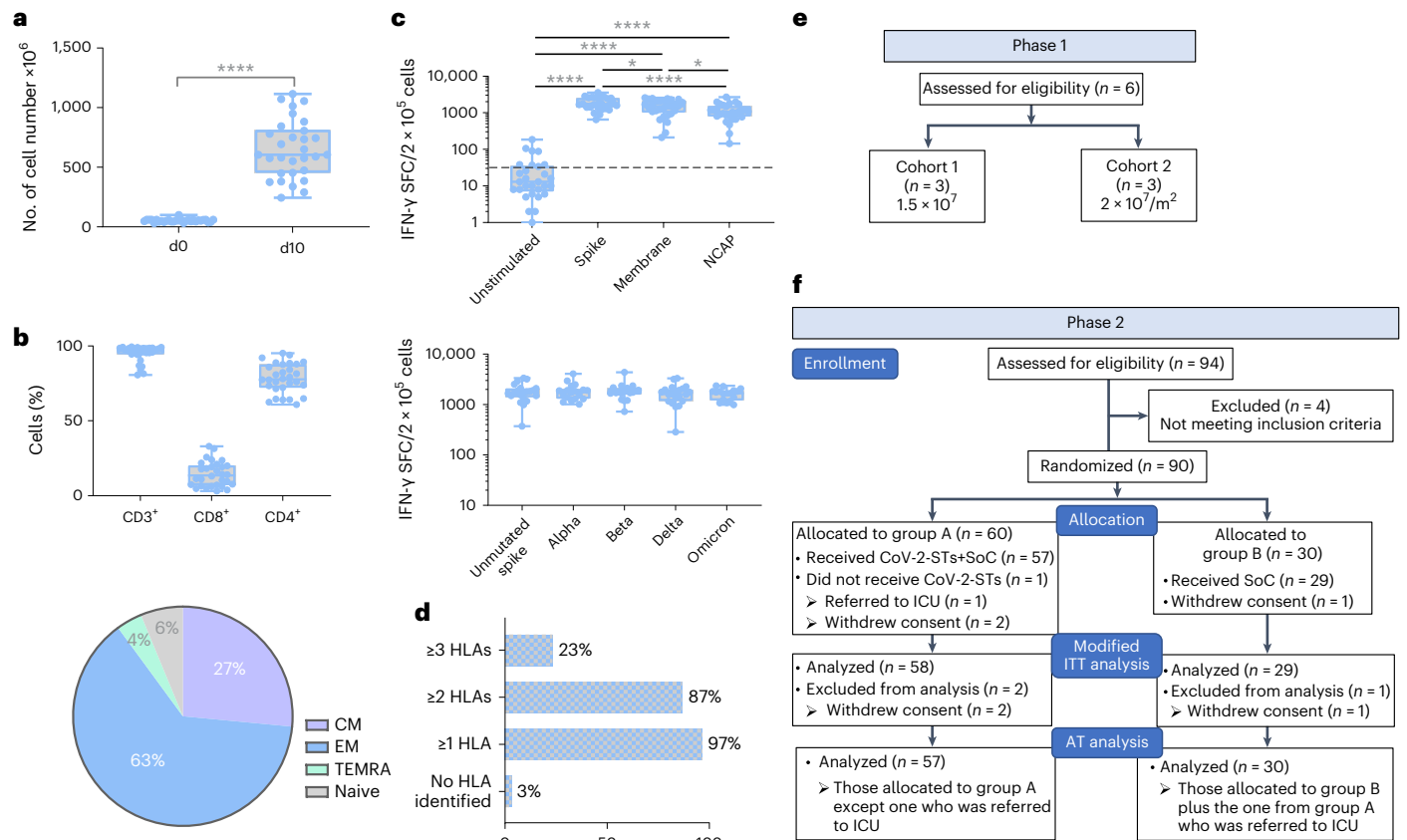


Fig. 1 | CoV-2-ST cell product characteristics (left panels) and flow chart of patient enrollment and randomization (right panels). **a**, Ex vivo expansion of CoV-2-STs. Absolute cell numbers obtained after a 10-d culture in G-Rex bioreactors. Each dot represents a single T cell product ($n = 30$). Differences between datasets were analyzed using two-tailed t -test (**** $P < 0.0001$). **b**, Immunophenotype of CoV-2-STs (upper panel). Each dot represents a single T cell product ($n = 30$). Pie chart of lymphocyte subpopulation frequencies (lower panel). CD3⁺CD45RA⁺CD62L⁺ (EM); CD3⁺CD45RA⁺CD62L⁻ (CM); CD3⁺CD45RA⁺CD62L⁻ and TEMRA; CD3⁺CD45RA⁺CD62L⁻. **c**, Specificity of CoV-2-STs. IFN- γ -secreting CoV-2-STs upon stimulation with the spike, NCAP and membrane antigens (upper panel, $n = 30$) or with the unmutated SARS-CoV-2

spike antigen compared to its Alpha, Beta, Delta and Omicron variants (lower panel, $n = 18$). Each dot represents a single T cell product. P values were calculated using ordinary one-way ANOVA with FDR multiple testing corrections using the two-stage step-up method from Benjamini, Krieger and Yekutieli ($^*P < 0.05$ and $q < 0.05$). FDR-adjusted $^*P < 0.05$ and **** $P < 0.0001$. For all box plots, the center line corresponds to the median value; the lower and upper hinges correspond to the first and third quartiles (25th and 75th percentiles); and the whiskers extend from the largest to the smallest value. **d**, Number of HLA(s) mediating CoV-2-ST specificity of the T cell products ($n = 30$). **e**, Patient allocation to the tested doses during phase 1. **f**, Patient allocation during phase 2 and according to mITT and AT analyses.

CoV-2-STs as a ‘living drug’ for high-risk hospitalized patients with COVID-19 in a randomized clinical trial, conducted during the SARS-CoV-2 Delta variant prevalence in Greece and at a time before the approval of Paxlovid.

Results

Establishment of a CoV-2-ST cell bank

Thirty clinical-grade CoV-2-ST cell products were manufactured in the Good Manufacturing Practice (GMP) facility of George Papanikolaou Hospital from COVID-19 convalescent healthcare professionals, selected to express the most frequent human leukocyte antigen (HLA) molecules in the Greek population. Donor characteristics are summarized in Supplementary Table 1. Starting from 3–10 × 10⁷ peripheral blood mononuclear cells (PBMCs) and after pulsing with overlapping peptides spanning three immunogenic SARS-CoV-2 antigens (spike, membrane and nucleocapsid (NCAP)), we generated multiple clinical doses per donor, reaching median (×10⁷) 60.5 (range, 24.5–111.5) cells per product and 12-fold expansion (Fig. 1a). The cell products were polyclonal, almost exclusively T cells (median (%) 97 (range, 81–99)), enriched in CD4⁺ cells (median (%) 78 (range, 61–95)) but also containing CD8⁺ (median (%) 14 (range, 3–33)) cells. They also

expressed central memory (CM) and predominantly effector memory (EM) markers ((CD45RA⁺CD62L⁺ and CD45RA⁻CD62L⁻, respectively; Fig. 1b)), the latter representing an important feature for prompt immunologic response and low risk of graft-versus-host disease (GvHD)²². All CoV-2-ST products demonstrated robust specificity not only against the unmutated SARS-CoV-2 variant with spike being on the top of immunodominance hierarchy but, notably, also against the Alpha, Beta, Delta and Omicron spike variants (Fig. 1c and Supplementary Table 1). When SARS-CoV-2 functional responses were mapped for each product by HLA-restricted viral epitopes, at least one HLA mediating CoV-2-ST specificity was identified in 29 of 30 products (Fig. 1d).

Phase 1 results

The clinical safety of CoV-2-STs was assessed in six patients with COVID-19 at George Papanikolaou Hospital, during a dose-escalation, phase 1 study, by intravenously administering 1.5 × 10⁷ total or 2 × 10⁷/m² CoV-2-STs, along with SoC (Fig. 1e). The objectives of the phase 1 study were safety and tolerability, including determination of the maximum tolerated dose of CoV-2-STs. A 12-d interval was anticipated before next patient enrollment. Patients were of median age 54 years (95% confidence interval (CI) 45–70), and all but one had at least

one comorbidity (Supplementary Table 2). In one patient, COVID-19 developed 20 d after monodose vaccination. At the time of infusion, two patients were on nasal prongs, three on Venturi mask 40–60% and one on high-flow oxygen. All had pneumonia by X-ray or computed tomography (CT) imaging (Supplementary Table 2). There were no infusion-related dose-limiting toxicities, including cytokine release syndrome (CRS) and GvHD, at any dose level; thus, the $2 \times 10^7/m^2$ CoV-2-STs was defined as the final dose. Five of six patients recovered (≤ 3 by eight-category ordinal scale (OS)), for whom the median time to recovery, discharge from the hospital and negative molecular testing were 11 d, 11 d and 14 d, respectively (95% CI 5–12, 5–12 and 9–25) (Supplementary Table 2). Clinical recovery was associated with oxygen independence, considerable decrease of inflammatory marker serum levels and T cell lymphopenia recovery as early as median day 5 (95% CI 4–8) (Supplementary Table 2 and Supplementary Fig. 1a–c). Moreover, by excluding the vaccinated patient in whom high endogenous CoV-2-STs existed already at the time of infusion, in the four non-vaccinated patients in a post hoc analysis, recovery was associated with considerable expansion of circulating CoV-2-STs (spot-forming cells (SFCs)/ 5×10^5 PBMCs: day 0, median 17 (0–42); day 10, median 845 (275–1,200), $P = 0.025$ (Supplementary Fig. 1d)).

The sixth patient, on Venturi mask at the time of infusion, developed increasing oxygen needs, being ultimately intubated with acute respiratory distress syndrome (ARDS) 7 d after infusion while she remained hospitalized during the 60 d of follow-up. ARDS was accompanied by a ~ 10 -fold increase of D-dimers over baseline and non-clinically relevant elevation of pro-inflammatory cytokines (Supplementary Table 3), suggesting its possible association with COVID-19 rather than the infused CoV-2-STs. Of note, that patient presented a delayed recovery of lymphopenia (day 14) and failed to expand CoV-2-STs (Supplementary Fig. 1c,d).

Phase 2 results

Patients. We screened 94 hospitalized patients with COVID-19 for eligibility at George Papanikolaou Hospital and Hippokrateion Hospital in Thessaloniki, Greece (Methods). Of these, 90 met the inclusion criteria and were randomly assigned (2:1) to receiving either CoV-2-STs+SoC (arm A) or SoC only (arm B). Three patients withdrew consent, and one patient (patient (Pt) 83), who was initially allocated to the CoV-2-STs+SoC cohort, was intubated before receiving the cells. Here we present the modified intention-to-treat (mITT) analysis as primary analysis²³, including all finally consented (three patients withdrew consent before day 0) and randomized patients (arm A: 58; arm B: 29), and the as-treated (AT) analysis as secondary analysis (arm A: 57; arm B: 30) (Fig. 1f). Notably, a suitable CoV-2-ST product was identified for all patients in arm A, and 56/57 patients who received CoV-2-STs were sharing at least one HLA-DRB1 with the cellular product.

In the total cohort, with a median age of 57 years (interquartile range, 50–67), 21% of the patients were vaccinated; 40% were female; 85% had a Karnofsky score (KS) between 50 and 80; 48% had a high need for oxygen supply due to severely impaired respiratory function; and more than half had at least two comorbidities. Baseline demographic and disease characteristics were well balanced between the two groups, the only exception being that the incidence of diabetes was higher in the SoC arm. None of the enrolled patients had previously been exposed to SARS-CoV-2. The median time from symptom onset or consent to day 0 was 5 d (maximum 6 d) and 2 d (maximum 3 d), respectively, in both arms (Table 1).

Safety outcomes. All infusions were well tolerated, without any immediate toxicities. There was not a single case of acute GvH reaction. Skin manifestations in one patient in arm A presenting as erythematous/morbiliform eruptions (Supplementary Fig. 2) were considered as a COVID-associated rash and resolved without specific treatment. CRS, a severe inflammatory response accompanied by hypoxia and

usually associated with the use of chimeric antigen receptor (CAR) T cells—albeit rare with non-genetically engineered T cells—has also been described in patients with severe COVID-19, usually in the form of ARDS. Differential diagnosis of such a rare but possible antigen-specific T-cell-associated CRS from a COVID-19-associated CRS was based on monitoring and assessment of specific biomarkers²⁴ (Methods and Supplementary Table 4). On this basis, ARDS in all patients met the criteria of a SARS-CoV-2-related serious adverse event (SAE).

In total, 12 of 57 (21%) and 11 of 30 (37%) of patients in arm A and arm B, respectively, presented with or developed over time elevated cytokine levels. Notably, 10–20 d after day 0, three of 30 (Pt-33, Pt-53 and Pt-73) SoC patients (10%) and only one of 57 (Pt-48) CoV-2-ST+SoC patients (1.75%) still maintained IL-6 levels of more than 1,000 pg ml⁻¹ (Fig. 2a). Day 10 serum IL-6 and TNF- α levels were overall higher in the SoC patients compared to the CoV-2-STs+SoC patients ($P = 0.03$ and $P = 0.026$, respectively; Fig. 2b). Tocilizumab was administered (Pt-48) at the clinicians' discretion. These data indicate that CoV-2-STs not only did not induce CRS but also largely controlled the SARS-CoV-2-triggered systemic inflammatory reaction.

No statistically significant difference was observed in the incidence of adverse events (AEs) between the two study arms, with the exception of a higher rate of increased international normalized ratio (INR) in the SoC arm ($P = 0.045$; Extended Data Table 1). The most common AEs occurring after day 0 in at least 2% of patients in either group were anemia, neutropenia, platelets decrease, elevation of liver enzymes, hypoalbuminemia and diarrhea. Grade 3 or 4 AEs occurred in 17 patients (29.8%) in the treatment group and in 14 patients (46.7%) in the control group. The most common grade 3 or 4 AEs occurring in at least 5% of all patients were anemia, hypoalbuminemia and thrombocytopenia. SAEs in the form of any-grade ARDS developed in 19 patients in the CoV-2-ST+SoC arm (33.3%) and in 15 patients in the SoC arm (50%) ($P = 0.13$), which is a significant difference when ARDS grade 5 was considered (21% versus 40%, respectively, $P = 0.05$). Likewise, grade 5 sepsis was less commonly seen in the CoV-2-STs+SoC group compared to the SoC group (12.3% versus 30%, respectively, $P = 0.04$). Of the total 14 deaths in the treatment group, none was deemed by the investigators to be related to the trial regimen (Extended Data Table 1).

Clinical responses. Primary efficacy outcome, time to recovery and recovery rate. Sixty-five percent (37/57) of CoV-2-STs+SoC-treated patients met the criteria of recovery by day 30 versus 38% (11/29) of SoC-treated patients ($P = 0.017$; Table 2). The median time to recovery from day 0 was 11 d for CoV-2-ST-treated patients, whereas it was not reached (NR) for SoC-treated patients ($P = 0.052$), with a rate ratio for recovery of 1.71 (95% CI 1.03–2.83; $P = 0.036$ and crude hazard ratio (HR) of 1.96 (95% CI 0.98–3.90; $P = 0.055$)) (Fig. 3a, Supplementary Fig. 3a, Table 2 and Supplementary Table 5). An analysis adjusting for age (≥ 55 years and < 55 years), KS and vaccination as covariates to evaluate the effect on the primary outcome did not indicate significant superiority of the CoV-2-STs+SoC treatment across the subgroups (Supplementary Fig. 3b,c).

Co-primary efficacy outcome and expansion of CoV-2-STs. CoV-2-ST longitudinal data were analyzed in response to arm and vaccination status up to 22 d after infusion, and both of these variables were shown to affect CoV-2-ST kinetics (Fig. 3b and Supplementary Fig. 4a). Specifically, patients in arm A exhibited significantly higher numbers of circulating CoV-2-STs for up to 22 d after infusion compared to patients in arm B (post hoc Tukey test, $P = 0.048$; Fig. 3b), whereas baseline values did not differ significantly (Mann–Whitney test, $P = 0.553$; Supplementary Fig. 5). However, when extending the follow-up time to 60 d, differences between patients in each arm were attenuated (post hoc Tukey test, $P = 0.183$; Fig. 3c and Supplementary Fig. 4b). These data suggest that the CoV-2-ST treatment triggered an earlier reconstitution of SARS-CoV-2-specific immunity in patients in arm A, potentially

Table 1 | Baseline characteristics of study participants (mITT population)

Summary statistics (baseline)	Group A	Group B	P value
	n=58	n=29	
Age (years)			
Mean (s.d.)	56.7 (11.9)	59.3 (9.7)	0.311 ^a
Median (Q1–Q3)	56.0 (48.0–66.0)	60 (51.0–67.0)	
Sex, n (%)			
Males	35 (60.3%)	17 (58.6%)	0.877 ^b
Females	23 (39.7%)	12 (41.4%)	
Time from first symptom to day 0 (days)			
Median (Q1–Q3)	5 (3–6)	5 (4–6)	0.754 ^c
Time from consent to day 0 (days)			
Median (Q1–Q3)	2 (2–3)	2 (2–2)	0.185 ^c
WHO OS at day 0, n (%)			
OS 3	3 (5.2%)	0 (0.0%)	0.179 ^c
OS 4	48 (82.8%)	22 (75.9%)	
OS 5	6 (10.3%)	7 (24.1%)	
OS 6	1 (1.7%)	0 (0.0%)	
Oxygen supply, n (%)			
No	3 (5.2%)	0 (0.0%)	0.548 ^c
Yes	55 (94.8%)	29 (100.0%)	
Oxygen supply specification, n (%)			
Nasal cannula	19 (33.9%)	8 (26.7%)	0.306 ^c
Venturi mask 35%	1 (1.8%)	0 (0.0%)	
Venturi mask 40%	2 (3.6%)	2 (6.9%)	
Venturi mask 60%	10 (17.9%)	2 (6.9%)	
Non-rebreather mask	15 (26.8%)	7 (24.1%)	
Non-rebreather mask ^b nasal cannula	1 (1.8%)	3 (10.3%)	
High-flow	5 (8.9%)	3 (10.3%)	
Non-invasive ventilation	2 (3.6%)	4 (13.8%)	
Intubation, mechanical ventilation	1 (1.8%)	0 (0.0%)	
Pneumonia by imaging			
No	0 (0%)	1 (3.4%)	0.558 ^b
Yes	57 (98.3%)	28 (96.6%)	
N/A	1 (1.7%)	0 (0%)	
Vaccination, n (%)			
No	48 (82.8%)	21 (72.4%)	0.261 ^b
Yes	10 (17.2%)	8 (27.6%)	
KS at day 0			
90–100	10 (17.2%)	3 (10.3%)	0.409 ^c
70–80	30 (51.8%)	13 (44.8%)	
50–60	18 (31.0%)	13 (44.8%)	
Comorbidities, n (%)			
No	12 (20.7%)	4 (13.8%)	0.562 ^c
Yes	46 (79.3%)	25 (86.2%)	
Number of comorbidities			
0	12 (20.7%)	4 (13.8%)	0.132 ^b
1	19 (32.8%)	6 (20.7%)	
2	15 (25.9%)	6 (20.7%)	
>2	12 (20.7%)	13 (44.8%)	

Table 1 (continued) | Baseline characteristics of study participants (mITT population)

Summary statistics (baseline)	Group A	Group B	P value
	n=58	n=29	
Comorbidities ^d , n (%)			
Blood malignancies—allogeneic HSCT transplantation	1 (1.7%)	0 (0.0%)	> 0.999 ^e
Cancer	4 (6.9%)	2 (6.9%)	> 0.999 ^e
Active	3 (5.2%)	0 (0.0%)	>0.999 ^e
Non-active	1 (1.7%)	2 (6.9%)	0.257 ^e
Cardiovascular disease/hypertension	22 (37.9%)	14 (48.3%)	0.356 ^b
Diabetes mellitus	8 (13.7%)	11 (37.9%)	0.010 ^b
Obesity	26 (44.8%)	9 (31.0%)	0.216 ^b
Neurological and psychiatric disorders	5 (8.6%)	2 (6.9%)	0.780 ^c
Renal disease	0 (0.0%)	1 (3.4%)	0.333 ^c
Autoimmune disease	1 (1.7%)	2 (6.9%)	0.257 ^c
Respiratory disease	2 (3.5%)	3 (10.0%)	0.328 ^c
Smoking currently	1 (1.7%)	2 (6.9%)	0.257 ^c
Other	10 (17.2%)	6 (20.7%)	0.696 ^b

Q1, 1st quartile; Q3, 3rd quartile; WHO, World Health Organization. ^aTwo-sample t-test with equal variances. Heteroskedasticity was evaluated with Levene's test. ^bPearson's chi-square test ^clog-rank test ^dEach patient could have more than one. ^eFisher's exact test ^fAll statistical tests were two-sided. All patients were Caucasians.

providing a recovery advantage, whereas, not unexpectedly, at later time points, the endogenous CoV-2-ST immunity eventually developed in recovering patients in arm B.

A further exploratory analysis showed that vaccination before COVID-19 resulted in significantly increased circulating CoV-2-STs compared to unvaccinated status throughout the entire study duration (post hoc Tukey test, $P = 0.008$ at 22 d of follow-up and $P = 0.019$ at 60 d of follow-up; Fig. 3b,c). Notably, this effect on hybrid immunity was further boosted by CoV-2-ST infusion during the breakthrough infection, as, early on (day 10), CoV-2-STs in vaccinated CoV-2-ST+SoC-treated patients were considerably higher than in their SoC-treated counterparts and healthy vaccinees ($q \leq 0.021$; Fig. 3d).

Key secondary endpoint: survival. The median time to death was NR and 53 d in the CoV-2-ST+SoC and SoC patients, respectively ($P = 0.007$; Table 2 and Supplementary Table 5) with 53% lower day 60 mortality risk in those receiving the CoV-2-STs infusion (24.1% versus 51.7%; risk ratio (RR) 0.47; 95% CI 0.26–0.83; $P = 0.01$). The day 60 crude HR demonstrated an approximately 62% lower hazard for death, in favor of T lymphocyte infusion (HR (95% CI) 0.38 (0.18–0.79), $P = 0.009$) (Fig. 4a, Supplementary Fig. 6, Table 2 and Supplementary Table 5). The difference in survival between the two arms could be seen already from day 30 (Table 2 and Extended Data Fig. 1). In a stratified post hoc subgroup analysis, CoV-2-ST+SoC-treated patients aged ≥ 50 years and the unvaccinated CoV-2-ST+SoC recipients were favored in terms of mortality compared to those receiving SoC only (HR (95% CI), ≥ 50 years: 0.43 (0.20–0.91), $P = 0.028$; unvaccinated: 0.40 (0.18–0.90), $P = 0.026$) (Extended Data Fig. 2 and Supplementary Fig. 7). Vaccinated CoV-2-ST+SoC-treated patients presented low, albeit not statistically significant, mortality (1/10, 10%) compared to vaccinated SoC-treated patients (4/8, 50%; $P = 0.06$, chi-square test), probably due to the small overall number of vaccinees developing severe COVID-19 (18/87), to meet eligibility for the study (Supplementary Fig. 7 and Table 1). It is noteworthy, however, that the one vaccinated CoV-2-ST+SoC-treated patient who died was an allogeneic HSCT recipient, whereas, among vaccinated SoC patients, two of eight were

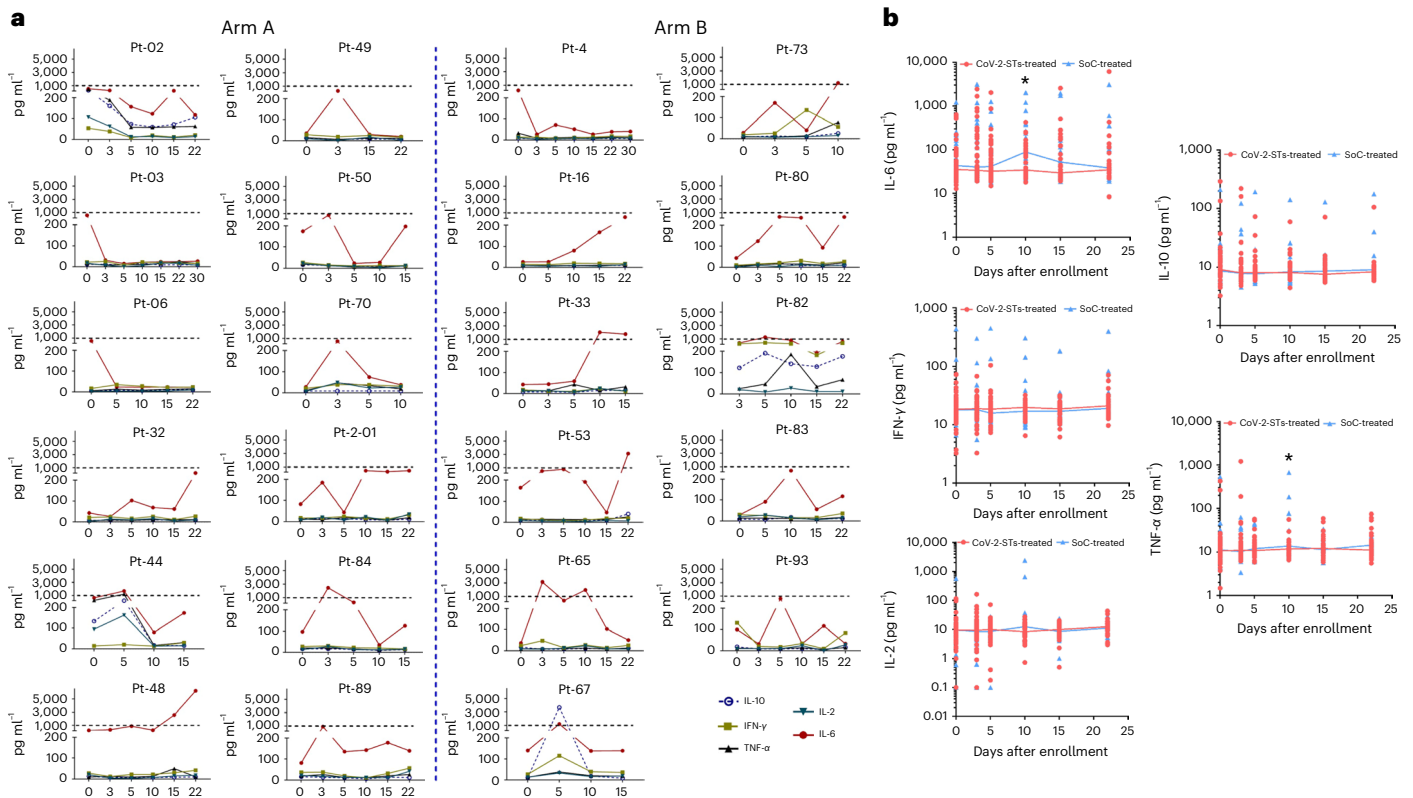


Fig. 2 | Safety of immunotherapy with CoV-2-STs. a, Serum cytokine levels in CoV-2-ST+SoC-treated patients (arm A, left panel, $n = 12/57$) and SoC-treated patients (arm B, right panel, $n = 11/30$) who either presented with or later developed increased cytokine levels. Each graph represents a single patient. The dotted line represents the 1,000-pg ml⁻¹ value. **b**, Cytokine levels of all CoV-2-

ST+SoC-treated patients (red, $n = 57$) and SoC-treated patients (blue, $n = 30$). Each dot represents a single patient. Lines display the median values. Differences between datasets were analyzed using the Mann-Whitney test, two-tailed. *P* values: IL-6, $P = 0.032$; TNF- α , $P = 0.026$.

receiving immunosuppression for autoimmune diseases, and four of eight had more than two comorbidities.

Secondary and exploratory endpoints. Immunological responses. Both innate and adaptive immunity reconstituted earlier in CoV-2-ST+SoC-treated patients (Fig. 4b,c). In particular, and apart from the earlier recovery of SARS-CoV-2-specific immunity, CoV-2-ST+SoC-treated patients also achieved faster reconstitution of CD3⁺ cells than SoC-treated patients and maintained higher numbers of CD3⁺ cells throughout the follow-up period (Tukey honestly significant difference (HSD) test, $P = 0.0024$) (Extended Data Fig. 3). Moreover, the CoV-2-ST+SoC treatment in previously vaccinated individuals (Fig. 4b) resulted in higher CD3⁺ numbers than in their SoC-treated counterparts (Tukey HSD adjusted $P = 0.0018$), whereas no difference between the arms was observed within the unvaccinated cohorts (Tukey HSD adjusted $P = 0.5649$). Natural killer (NK) cells are key players in maintaining immune homeostasis and are both quantitatively and qualitatively impaired in severe COVID-19 (refs. 25,26). We observed significant variation in NK kinetics associated with treatment and vaccination (Supplementary Fig. 4d). Patients treated with CoV-2-STs+SoC exhibited significantly higher NK numbers than SoC-treated patients (Tukey HSD $P = 0.049$; Fig. 4c), whereas no significant differences were observed at randomization (Mann-Whitney test, $P = 0.362$). Likewise, vaccinated patients with hybrid immunity also had higher NK numbers than the unvaccinated patients (Tukey HSD $P = 0.006$; Fig. 4c).

Patients in arm A presented a faster clearance of the viral load (slope *t*-test, $P = 0.0017$) than patients in control arm B (Fig. 4d), with 30% versus 20% of arm A and arm B patients becoming SARS-CoV-2-free by day 10, respectively (Mann-Whitney test, $P = 0.03$; Supplementary

Fig. 8). The longitudinal kinetics of viral load was highly and inversely correlated with the in vivo expansion of CoV-2-STs (Extended Data Fig. 4), thus suggesting that the delayed CoV-2-ST recovery in patients in arm B might have contributed to the prolonged viremia compared to patients in arm A, whereas the rapid expansion of CoV-2-STs in SoC-treated patients led to earlier SARS-CoV-2 clearance.

Humoral neutralizing responses were affected by previous vaccination and the combinatorial effect of CoV-2-ST treatment and previous vaccination. Vaccination alone explained most of the variance observed (ANOVA $F_{(1,320)} = 235.2740$, $P < 2.2 \times 10^{-16}$; Supplementary Fig. 4e), followed by its combinatorial effect with treatment arm (ANOVA $F_{(1,320)} = 5.1986$, $P = 0.023$; Supplementary Fig. 4e). Consequently, the vaccinated cohort exhibited significantly higher numbers of CoV-2 neutralizing antibodies (Nabs) over time than the non-vaccinated cohort (Tukey's HSD adjusted $P = 1.0487 \times 10^{-12}$), whereas vaccinated CoV-2-ST+SoC-treated patients displayed superior humoral responses over all other groups (Tukey HSD adjusted *P* value compared to vaccinated SoC-treated patients = 0.027) (Fig. 4e). Collectively, these data support that breakthrough COVID-19 infection after vaccination powers up the immune response over vaccination only or infection only and demonstrates that, in the context of hybrid immunity, CoV-2-STs, apart from T cell responses, also trigger humoral responses. In the context of natural immunity, however, CoV-2-STs do not boost CoV-2 Nabs in affected patients for at least 22 d after infusion (Fig. 4e).

Overall, and irrespective of the treatment arm, surviving patients presented robust cellular (CoV-2-STs, CD4⁺ and CD8⁺ cell subsets) and humoral (CoV-2 Nabs) immunological responses compared to patients who died, showing SARS-CoV-2-specific T cell responses to be a key player for the outcome²⁷ (Fig. 4f,g and Extended Data Fig. 5).

Table 2 | Median times to event and outcomes (mITT population)

	Group A (n=58)	Group B (n=29)	P value ^a	Total cohort, n=87
Status at day 30, n (%)				
Dead	10 (34.5%)	8 (13.8%)	0.025 ^b	18 (20.7%)
Status at last follow-up (day 60), n (%)				
Alive and well	37 (63.8%)	12 (41.4%)	0.047 ^b	49 (56.3%)
Alive with disease	7 (12.1%)	2 (6.9%)	0.455 ^b	9 (10.3%)
Dead	14 (24.1%)	15 (51.7%)	0.010 ^b	29 (33.3%)
Day 30 recovered patients / n (%)	(n=57) ^c 37 (64.9%)	11 (37.9%)	0.017 ^b	(n=86) 48 (55.8%)
Days to recovery (median, Q1–Q3)–day 30	(n=57) ^c 11 (6, NR)	NR (7, NR)	0.052 ^d	(n=86) 16 (6, NR)
Day 30 recovery rates / risk ratio (95% CI)	1.71 (1.03–2.83)		0.036 ^e	
HR (95% CI) through day 30	1.96 (0.98–3.90)		0.055 ^f	
Days to death (median, Q1–Q3)	NR (44, NR)	53 (19, NR)	0.007 ^d	NR (34, NR)
Day 30 mortality rates / risk ratio (95% CI)	0.40 (0.18–0.90)		0.028 ^e	
Day 60 mortality rates / risk ratio (95% CI)	0.47 (0.26–0.83)		0.010 ^e	
HR (95% CI) through day 30	0.35 (0.14–0.88)		0.026 ^f	
HR (95% CI) through day 60	0.38 (0.18–0.79)		0.009 ^f	
Length of hospitalization from day 0 (median days, Q1–Q3)	10 (5, 27)	16 (6, 34)	0.293 ^d	11 (6, 29)
Intubation				
Days to intubation (median, Q1–Q3)	NR (10, NR)	23 (5, NR)	0.088 ^d	NR (9, NR)
% of patients intubated	22/58 (37.9%)	15/29 (51.7%)	0.220 ^c	37/87 (42.5%)
% of patients extubated	8/22 (36.4%)	2/15 (13.3%)	0.153 ^c	10/37 (27.0%)

^aAll tests were not adjusted for multiple comparisons. ^bPearson's chi-square test ^c57 evaluable of 58 total patients. One patient had OS=3 on day 0 (time to event=0) and was excluded from the recovery rate analysis. ^dlog-rank test ^eWald statistic based on a logistic regression model ^fWald statistic based on a Cox model. All statistical tests were two-sided.

Other exploratory endpoints. SoC-treated-patients had a higher rate of intubation (15/29, 51.7% versus 22/58, 37.9%) and a lower rate of extubation (2/15, 13.3% versus 8/22, 36.4%) than CoV-2-ST+SoC-treated patients. The median time to intubation was NR for the treatment arm and was 23 d for the control arm ($P=0.088$). Hospitalization length, although shorter by 6 d in the CoV-2-ST+SoC group, did not reach significance (Table 2, Supplementary Table 5, Extended Data Fig. 6 and Supplementary Fig. 9). Overall, at the end of follow-up (day 60), the clinical status of patients favored enrollment in arm A, with higher rates

of CoV-2-ST+SoC-treated patients being alive and well (63.8% versus 41.4%, $P=0.047$) (Table 2 and Supplementary Table 5).

Donor DNA by microchimerism assay in ex vivo expanded patients' CoV-2-STs became apparent from day 5 (median 1.72% (range, 0–4.65%)), reaching peak levels on day 15 (median 2.63% (range, 1.03–39.63)). Although those CoV-2-STs were ex vivo expanded and do not reflect the actual frequency of donor-derived CoV-2-STs in patient PBMCs, the trend in the kinetics of total circulating CoV-2-STs and donor DNA over time may allude to an in vivo expansion of donor CoV-2-STs (Fig. 4h). Interestingly, and despite the partial HLA matching between recipients and donors (Supplementary Table 6), the infused CoV-2-STs persisted for at least 60 d (median 2.71% (range, 1.27–2.83)). The overall degree of HLA matching between the cell product and CoV-2-ST recipients or the HLA class did not affect donor microchimerism frequencies or survival (Supplementary Table 7 and Supplementary Fig. 10).

Biomarkers previously reported to be associated with poor outcome of severe COVID-19 (refs. 28,29) showed peak values at days 10–15 after randomization in both arms, reaching higher levels (C-reactive protein (CRP), ferritin, lactate dehydrogenase (LDH) and D-dimers) in the SoC-treated patients than in the CoV-2-STs+SoC-treated patients, yet without statistical significance ($P \geq 0.09$). Total white blood cells peaked on day 15, trending higher in the SoC arm ($P=0.066$; Supplementary Fig. 11).

Discussion

Dexamethasone⁵ and remdesivir⁶ have become the SoC in patients with COVID-19 with oxygen needs and moderate to severe illness, respectively. Recently, two oral anti-COVID-19 drugs, nirmatrelvir/ritonavir (Paxlovid) and molnupiravir, received authorization for the treatment of mild/moderate COVID-19 in outpatients at increased risk for progression to severe COVID-19 (refs. 1–3). Treatment options, however, for hospitalized patients with severe COVID-19 are limited, and no benefit of tested drugs in 'hard' endpoints, including survival^{30–32}, has been shown, with the exception of IL-6 receptor antagonists in the subpopulation of critically ill patients in the intensive care unit (ICU) under organ support⁴.

We and others have highlighted the major role of T cell immunity in COVID-19 resolution, demonstrating that lymphopenia is associated with poorer outcomes^{33–35}, whereas circulating CoV-2-STs in convalescent patients promote recovery and reduce disease severity^{21,36,37}. Given the paucity of therapeutic options and the key role of specific T cell immunity in severe COVID-19, along with the successful control of other viral infections with virus-specific T cells (VSTs) in the context of HSCT, we assessed the safety and efficacy of off-the-shelf CoV-2-STs compared to SoC in patients with severe COVID-19, before the Paxlovid era.

We generated a bank with convalescent donor-derived, highly specific CoV-2-STs against SARS-CoV-2 and its known variants, which were polyclonal, CD4⁺ cell predominant³⁸ and expressed CM and EM markers. In a previous, extensive immunophenotypic characterization, we demonstrated that CoV-2-STs exhibit an activated profile, lacking expression of T-regulatory and exhaustion markers²¹. Such CD4⁺ predominant responses against SARS-CoV-2, but against other respiratory viruses as well^{39,40}, have been described in the context of targeted immunotherapy, providing evidence that CD4⁺ responses are critical not only for efficient CD8⁺ cell and antibody response but also for direct killing of virus-infected cells and recruitment to the infection site of other immune cells by cytokine production^{41–43}.

The infusion of CoV-2-ST had an excellent safety profile, without inducing CRS or GvHD⁴⁴, in line with a recent pilot study from Baylor College of Medicine where the infusion of off-the-shelf CoV-2-STs in immunocompromised patients with COVID-19 proved safe and resolved the SARS-CoV-2 infection in three of four patients⁴⁵. Indeed, VSTs have a limited capacity to induce GvHD, being dominated by memory T cells with a limited T-receptor diversity,

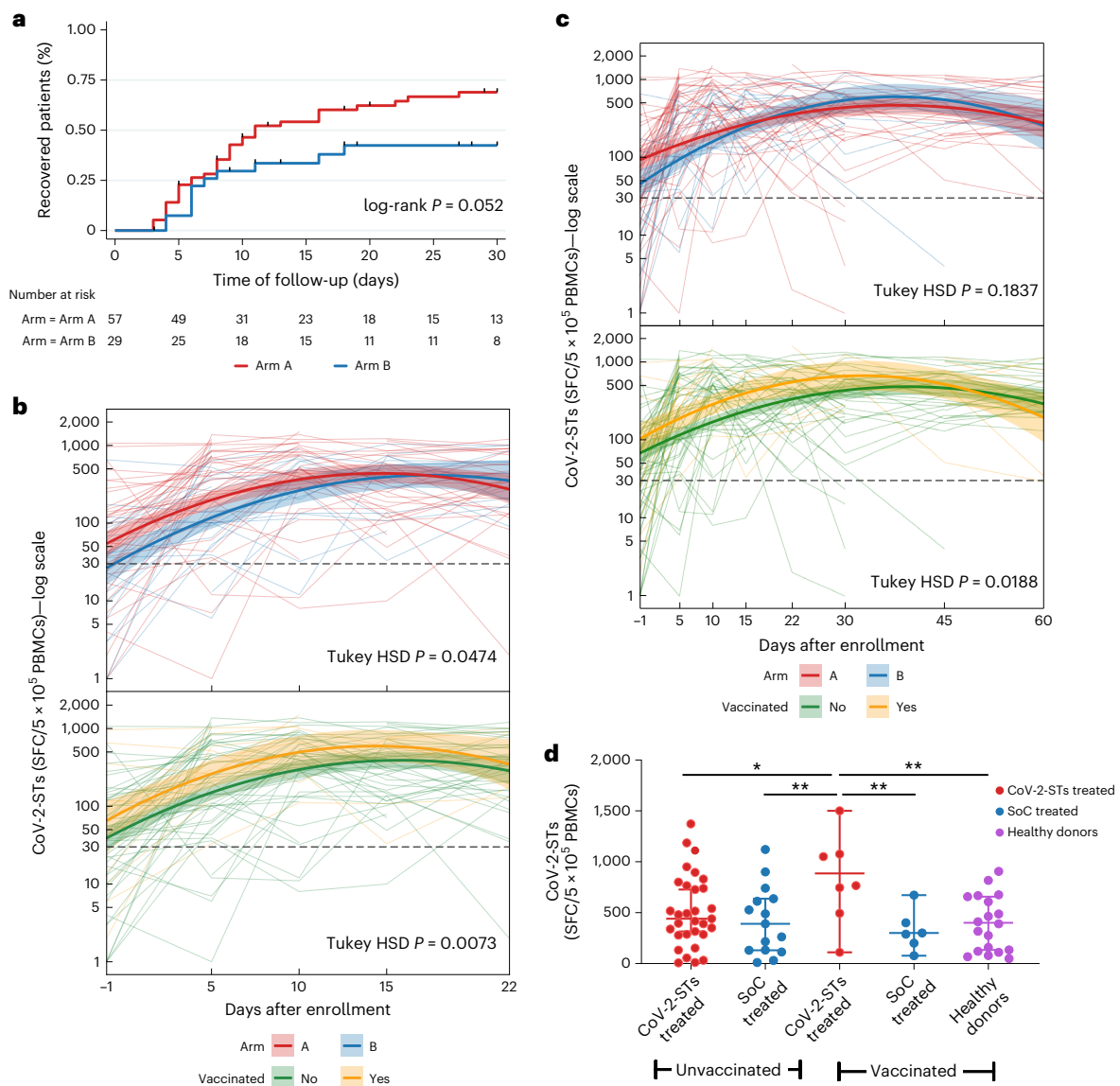


Fig. 3 | Primary efficacy outcomes. **a**, Kaplan–Meier curves for recovery (time to OS ≤ 3) at 30 d in the mITT population. **b,c**, Longitudinal trajectories of circulating CoV-2-STs in CoV-2-ST+SoC-treated patients (red lines, $n = 58$) and SoC-treated patients (blue lines, $n = 29$) and in vaccinated (yellow lines) and unvaccinated (green lines) patients through day 22 (**b**) and day 60 (**c**). Thin lines represent the values of circulating CoV-2-STs of each patient. Bold lines are the quadratic fitted splines of each arm. Shaded bands extend to 95% CI of the fitted values. The dashed horizontal line indicates the cutoff for CoV-2-ST specificity

(≥ 30 SFCs/5 $\times 10^5$ PBMCs). Tukey HSD test P values are reported. **d**, Day 10 values of circulating CoV-2-STs in vaccinated ($n = 8$) and unvaccinated ($n = 30$) CoV-2-ST+SoC-treated patients and SoC-treated patients ($n = 7$ and $n = 16$, respectively) and in healthy vaccinees ($n = 20$). Scatter plot indicates individual patient (dots); thick line is median; error bars represent 95% CI. P values were calculated using one-way ANOVA with FDR multiple testing corrections using the two-stage step-up method from Benjamini, Krieger and Yekutieli ($^*P < 0.05$ and $q < 0.1$). FDR-adjusted $^*P = 0.02$ and $^{**}P = 0.01$.

considered naturally occurring, ‘universal’ donor T cells²². CRS is also rare after VST infusion, as T cells express native receptors directed to tumor-associated or virus-associated antigens, generating more physiological antigen–receptor interactions than CAR T cells where CRS is triggered by the activation of tumor-directed T cells via artificial receptors^{46,47}.

Our trial population comprised real-world patients with severe Delta variant illness, as delineated by the eligibility criteria and baseline characteristics, with most having $KS \geq 50 \leq 80$ and at least two comorbidities. In this high-risk population, CoV-2-ST+SoC treatment resulted in increased recovery rates and a shorter time to recovery. After infusion, circulating CoV-2-STs significantly expanded through day 22, probably contributing to the increased early recovery rates and faster reduction of viral load (in correlation with CoV-2-ST kinetics) in

CoV-2-ST+SoC-treated patients compared to SoC-treated patients. The earlier restoration of SARS-CoV-2-specific immunity was also accompanied by faster recovery of both adaptive (CD3⁺ cells) and innate (NK cells) immunity and an overall attenuated inflammatory response during the critical days after randomization. A 53% reduced risk of mortality in the treatment group, although significant, should be interpreted with caution as multiplicity adjustments were not implemented.

Previously vaccinated patients developed hybrid immunity, generated by the additional antigen exposure through natural infection. Hybrid immunity induces greater humoral responses⁴⁸ and memory SARS-CoV-2-specific B cells and T cells⁴⁹. We show that, in this context of hybrid immunity, CoV-2-ST infusion further boosted both cellular and humoral responses, thus shaping a potentially protective ‘super immunity’.

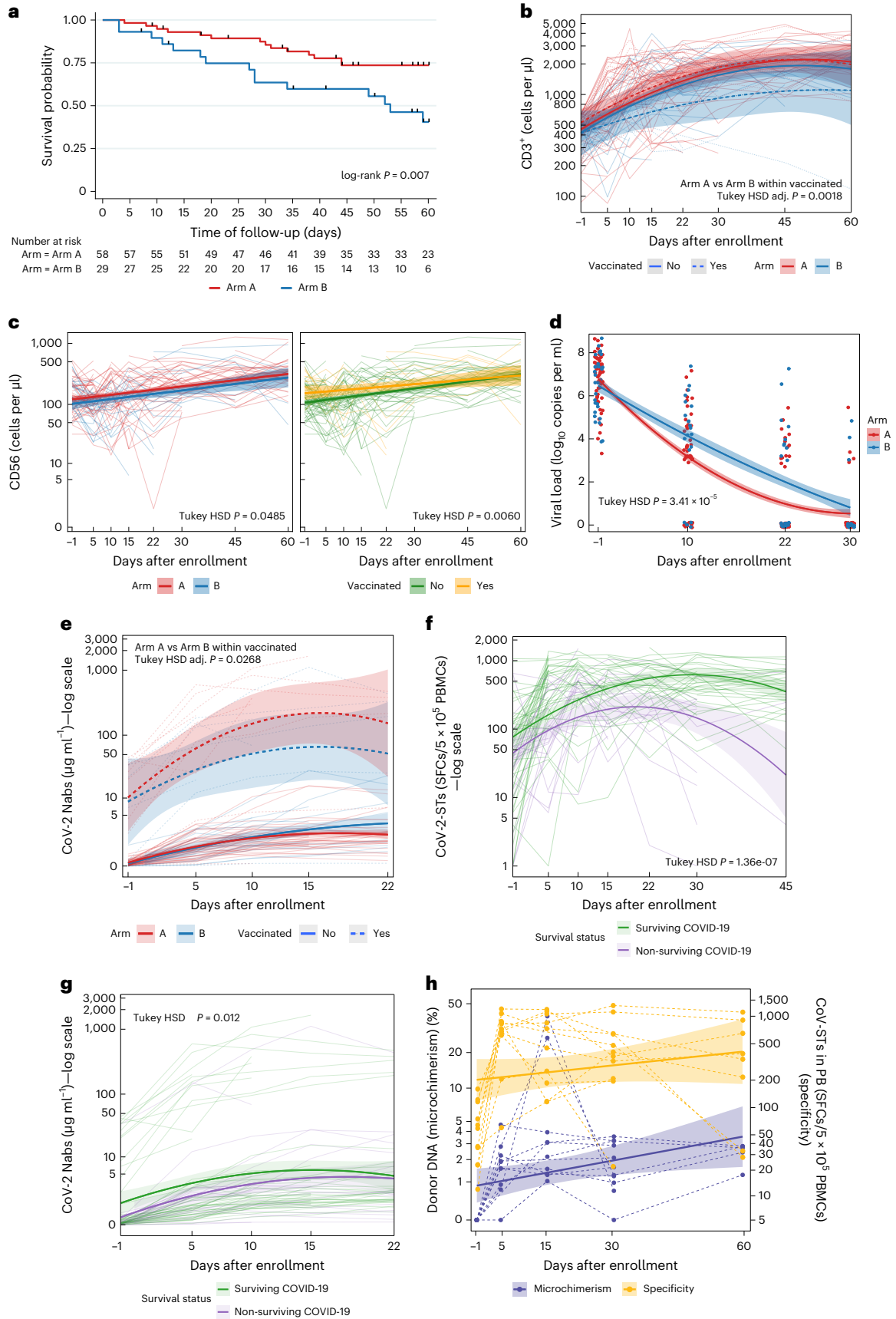


Fig. 4 | Secondary efficacy endpoints. **a**, Kaplan–Meier curves for mortality (time to death) at 60 d in the mITT population. **b,c**, Longitudinal trajectories of T lymphocytes (**b**) and NK cells (**c**, left panel) in CoV-2-ST+SoC-treated (red lines, $n = 58$) and SoC-treated (blue lines, $n = 29$) patients and longitudinal trajectories of NK cells (**c**, right panel) in vaccinated (yellow lines) or unvaccinated (green lines) patients. Thin lines represent the CD3⁺ or NK counts (cells per microliter) in individual patients. Bold lines are the quadratic fitted splines of each group. Shaded bands extend to 95% CI of fitted values. **d**, Longitudinal trajectories of viral load in CoV-2-STs+SoC-treated (red dots and lines, $n = 58$) and SoC-treated (blue dots and lines, $n = 30$) patients. Each dot represents an individual. Bold lines are the quadratic fitted splines of each arm. Shaded bands extend to 95% CI of fitted values. **e**, Kinetics of serum SARS-CoV-2 Nabs during follow-up time in CoV-2-STs+SoC-treated vaccinated (red dotted lines, $n = 10$), CoV-2-STs-treated unvaccinated (red solid lines, $n = 48$), SoC-treated vaccinated (blue dotted lines,

$n = 8$) and SoC-treated unvaccinated (blue solid lines, $n = 21$) patients. Thin lines represent the CoV-2-ST values of each CoV-2-ST+SoC-treated or SoC-treated patient. Bold lines are the quadratic fitted splines of each arm. Shaded bands extend to 95% CI of fitted values. **f,g**, Kinetics of circulating CoV-2-STs (**f**) and serum SARS-CoV-2 Nabs (**g**) in surviving (green lines, $n = 58$) and non-surviving (purple lines, $n = 29$) patients with COVID-19. Thin lines represent the CoV-2-ST values in individual patients. Bold lines are the quadratic fitted splines of each arm. Shaded bands extend to 95% CI of fitted values. **h**, Microchimerism as percent of donor DNA in patients' ex vivo expanded CoV-2-STs (left axis) and total circulating CoV-2-ST kinetics (right axis) during follow-up time. Dashed lines and points are kinetics for individual patients. Solid lines represent fitted values, and shaded bands extend to 95% CI of fitted values. y axes are log scaled. PB, peripheral blood.

A suitable product with ≥ 1 shared HLA mediating SARS-CoV-2 specificity could be found in all cases. Partially matched CoV-2-STs are expected to be eventually rejected by the host. Previous evidence in immunocompromised recipients suggested persistence of off-the-shelf VSTs or SARS-CoV-2-STs for at least 3 months or 6 months, respectively^{8,45,50}. Here, the infused CoV-2-STs were detected through the end of follow-up, 60 d after infusion, which, along with the higher CoV-2-ST trajectories at early timepoints after infusion and the faster CD3⁺ cell recovery in CoV-2-ST+SoC-treated patients, allowed us to speculate that donor CoV-2-STs may control the infection by being expanded early in vivo, boosting, in parallel, the endogenous T cell immunity.

Considering recipients of SARS-CoV-2-STs derived from donors exposed to a different SARS-CoV-2 variant, reasonable concerns may be raised about potential immune escape; however, our products, which were generated from wild-type virus-recovered donors and clinically used against the Delta variant, were cross-reactive to all known variants, including Omicron (Fig. 1c). Indeed, CoV-2-STs, by spanning the whole genome, have greater potential to conquer immune escape mutations than monoclonal antibodies, vaccines and recently the new antiviral drugs, the efficacy of which might be threatened by escape mutations in drug-binding motifs and imposed selective pressure^{51,52}.

Major strengths of our trial include the enrollment of real-world, high-risk patients and the ability to identify a suitable cell product for all patients under investigational treatment. Our study also has limitations, which should be considered when interpreting the results. The trial was powered only for the composite endpoint of recovery rate/time to recovery and not for the expansion of CoV-2-STs, owing to the absence at that time of any pre-existing data on the effect size for CoV-2-ST expansion in patients with COVID-19. As a phase 1/2 trial, it was not powered to assess the secondary endpoints, including the key secondary objective of survival by day 60, for which the widths of the CIs have not been adjusted for multiple testing and cannot infer definitive treatment effects. In addition, given the sample size, patient heterogeneity, especially in terms of vaccination and comorbidities, although balanced between the two groups, limited the ability to detect significant treatment effects in subgroup comparisons.

Another limitation is the initiation of treatment within a maximum of 7 d from symptom onset, not permitting evaluation at later stages of illness. The T cell intervention within this timeframe was decided on the basis that it typically takes a few days for T cells to expand, and the infusion cannot be performed earlier than the next day of randomization owing to the need for HLA typing; thus, the earliest possible intervention could mount a strong immune response before the critical second week of illness.

We also acknowledge that Paxlovid, as an early treatment within 5 d of symptom onset, will probably change the natural history of COVID-19 and limit the number of patients who would need alternative treatments, thus challenging the role of adoptive immunotherapy in

COVID-19 treatment. Nevertheless, the stringent eligibility criteria of our trial delineated a patient population that had, by day 5 after symptom onset, severe illness already (T-lymphopenia (87/87) and pneumonia (85/86 evaluable)), probably most not being eligible for Paxlovid today and in whom CoV-2-ST+SoC treatment potentially altered a possible adverse outcome.

In the new era of COVID-19 treatment, we anticipate that patients eligible for adoptive immunotherapy would be those who initially present with severe disease and oxygen needs; those who progress, develop resistance or experience severe breakthrough infection while on or after Paxlovid^{51–53}; or immunocompromised patients who develop prolonged viral shedding and may favor the selection of 'fitter' variants and in whom the prolonged persistence of off-the-shelf CoV-2-STs may enable virus clearance.

Our study suggests a feasible approach, without evident safety concerns, to adoptively transfer a 'natural' robust immunological memory for specific protection against severe COVID-19 across all known variants through convalescent donor CoV-2-ST infusions, which, when initiated within a maximum of 7 d after the onset of symptoms, led to improved recovery rates and non-conclusive evidence of reduced mortality. Future, larger phase 3 studies are needed to solidify the evidence that adoptive immunotherapy for severe COVID-19 has a key role to play and to justify the consideration of VSTs as a potential therapeutic platform for future emerging pandemic threats.

Online content

Any methods, additional references, Nature Portfolio reporting summaries, source data, extended data, supplementary information, acknowledgements, peer review information; details of author contributions and competing interests; and statements of data and code availability are available at <https://doi.org/10.1038/s41591-023-02480-8>.

References

1. Hammond, J. et al. Oral nirmatrelvir for high-risk, nonhospitalized adults with Covid-19. *N. Engl. J. Med.* **386**, 1397–1408 (2022).
2. Owen, D. R. et al. An oral SARS-CoV-2 M^{pro} inhibitor clinical candidate for the treatment of COVID-19. *Science* **374**, 1586–1593 (2021).
3. Jayk Bernal, A. et al. Molnupiravir for oral treatment of Covid-19 in nonhospitalized patients. *N. Engl. J. Med.* **386**, 509–520 (2022).
4. Gordon, A. et al. Interleukin-6 receptor antagonists in critically ill patients with Covid-19. *N. Engl. J. Med.* **384**, 1491–1502 (2021).
5. Horby, P. et al. Dexamethasone in hospitalized patients with Covid-19. *N. Engl. J. Med.* **384**, 693–704 (2021).
6. Beigel, J. H. et al. Remdesivir for the treatment of Covid-19—final report. *N. Engl. J. Med.* **383**, 1813–1826 (2020).
7. Papadopoulou, A. et al. Activity of broad-spectrum T cells as treatment for AdV, EBV, CMV, BKV, and HHV6 infections after HSCT. *Sci. Transl. Med.* **6**, 242ra83 (2014).

8. Tzannou, I. et al. Off-the-shelf virus-specific T cells to treat BK virus, human herpesvirus 6, cytomegalovirus, Epstein–Barr virus, and adenovirus infections after allogeneic hematopoietic stem-cell transplantation. *J. Clin. Oncol.* **35**, 3547–3557 (2017).
9. O’Reilly, R. J., Prockop, S., Hasan, A. N., Koehne, G. & Doubrovina, E. Virus-specific T-cell banks for ‘off the shelf’ adoptive therapy of refractory infections. *Bone Marrow Transplant.* **51**, 1163–1172 (2016).
10. Jiang, W. et al. Pathogen-specific T cells beyond CMV, EBV and adenovirus. *Curr. Hematol. Malign. Rep.* **14**, 247–260 (2019).
11. Kaeuferle, T., Krauss, R., Blaeschke, F., Willier, S. & Feuchtinger, T. Strategies of adoptive T-cell transfer to treat refractory viral infections post allogeneic stem cell transplantation. *J. Hematol. Oncol.* **12**, 13 (2019).
12. Baugh, K. A., Tzannou, I. & Leen, A. M. Infusion of cytotoxic T lymphocytes for the treatment of viral infections in hematopoietic stem cell transplant patients. *Curr. Opin. Infect. Dis.* **31**, 292–300 (2018).
13. Papadopoulou, A., Alvanou, M., Karavalakis, G., Tzannou, I. & Yannaki, E. Pathogen-specific T cells: targeting old enemies and new invaders in transplantation and beyond. *Hemasphere* **7**, e809 (2023).
14. Kim, N. et al. Off-the-shelf partial HLA matching SARS-CoV-2 antigen specific T cell therapy: a new possibility for COVID-19 treatment. *Front. Immunol.* **12**, 5562 (2021).
15. Keller, M. D. et al. SARS-CoV-2 specific T-cells are rapidly expanded for therapeutic use and target conserved regions of membrane protein. *Blood* **136**, 2905–2917 (2020).
16. Kedzierska, K. & Thomas, P. G. Count on us: T cells in SARS-CoV-2 infection and vaccination. *Cell Rep. Med.* **3**, 100562 (2022).
17. Ferreras, C. et al. SARS-CoV-2-specific memory T lymphocytes from COVID-19 convalescent donors: identification, biobanking, and large-scale production for adoptive cell therapy. *Front. Cell Dev. Biol.* **9**, 293 (2021).
18. Cooper, R. S. et al. Rapid GMP-compliant expansion of SARS-CoV-2-specific T cells from convalescent donors for use as an allogeneic cell therapy for COVID-19. *Front. Immunol.* **11**, 598402 (2021).
19. Leung, W. et al. Rapid production of clinical-grade SARS-CoV-2 specific T cells. *Adv. Cell Gene Ther.* **3**, e101 (2020).
20. Moss, P. The T cell immune response against SARS-CoV-2. *Nat. Immunol.* **23**, 186–193 (2022).
21. Papayanni, P.-G. et al. Vaccinated and convalescent donor-derived severe acute respiratory syndrome coronavirus 2-specific T cells as adoptive immunotherapy for high-risk coronavirus disease 2019 patients. *Clin. Infect. Dis.* **73**, 2073–2082 (2021).
22. Anderson, B. E. et al. Memory CD4⁺ T cells do not induce graft-versus-host disease. *J. Clin. Invest.* **112**, 101–108 (2003).
23. Schulz, K. F., Altman, D. G. & Moher, D. CONSORT 2010 statement: updated guidelines for reporting parallel group randomised trials. *BMJ* **340**, 698–702 (2010).
24. Leisman, D. E. et al. Cytokine elevation in severe and critical COVID-19: a rapid systematic review, meta-analysis, and comparison with other inflammatory syndromes. *Lancet Respir. Med.* **8**, 1233–1244 (2020).
25. Narni-Mancinelli, E. & Vivier, E. Clues that natural killer cells help to control COVID. *Nature* **600**, 226–227 (2021).
26. Wei, R. et al. A landscape study on COVID-19 immunity at the single-cell level. *Front. Immunol.* **13**, 918383 (2022).
27. Barouch, D. H. Covid-19 vaccines—immunity, variants, boosters. *N. Engl. J. Med.* **387**, 1011–1020 (2022).
28. Antunez Muiños, P. J. et al. The COVID-19 lab score: an accurate dynamic tool to predict in-hospital outcomes in COVID-19 patients. *Sci. Rep.* **11**, 9361 (2021).
29. Huang, I., Pranata, R., Lim, M. A., Oehadian, A. & Alisjahbana, B. C-reactive protein, procalcitonin, D-dimer, and ferritin in severe coronavirus disease-2019: a meta-analysis. *Ther. Adv. Respir. Dis.* **14**, 1753466620937175 (2020).
30. Stone, J. H. et al. Efficacy of tocilizumab in patients hospitalized with Covid-19. *N. Engl. J. Med.* **383**, 2333–2344 (2020).
31. Hermine, O. et al. Effect of tocilizumab vs usual care in adults hospitalized with COVID-19 and moderate or severe pneumonia: a randomized clinical trial. *JAMA Intern. Med.* **181**, 32–40 (2021).
32. Cao, B. et al. A trial of lopinavir–ritonavir in adults hospitalized with severe Covid-19. *N. Engl. J. Med.* **382**, 1787–1799 (2020).
33. Chen, G. et al. Clinical and immunological features of severe and moderate coronavirus disease 2019. *J. Clin. Invest.* **130**, 2620–2629 (2020).
34. Zhou, R. et al. Acute SARS-CoV-2 infection impairs dendritic cell and T cell responses. *Immunity* **53**, 864–877 (2020).
35. Yang, X. et al. Clinical course and outcomes of critically ill patients with SARS-CoV-2 pneumonia in Wuhan, China: a single-centered, retrospective, observational study. *Lancet Respir. Med.* **8**, 475–481 (2020).
36. Le Bert, N. et al. Highly functional virus-specific cellular immune response in asymptomatic SARS-CoV-2 infection. *J. Exp. Med.* **218**, e20202617 (2021).
37. Rydzynski Moderbacher, C. et al. Antigen-specific adaptive immunity to SARS-CoV-2 in acute COVID-19 and associations with age and disease severity. *Cell* **183**, 996 (2020).
38. Sekine, T. et al. Robust T cell immunity in convalescent individuals with asymptomatic or mild COVID-19. *Cell* **183**, 158–168 (2020).
39. Tzannou, I. et al. Immunologic profiling of human metapneumovirus for the development of targeted immunotherapy. *J. Infect. Dis.* **216**, 678–687 (2017).
40. McLaughlin, L. P. et al. Human parainfluenza virus-3 can be targeted by rapidly ex vivo expanded T-lymphocytes. *Cytotherapy* **18**, 1515 (2016).
41. McKinstry, K. K. et al. Memory CD4⁺ T cells protect against influenza through multiple synergizing mechanisms. *J. Clin. Invest.* **122**, 2847–2856 (2012).
42. Wilkinson, T. M. et al. Preexisting influenza-specific CD4⁺ T cells correlate with disease protection against influenza challenge in humans. *Nat. Med.* **18**, 274–280 (2012).
43. Swain, S. L., McKinstry, K. K. & Strutt, T. M. Expanding roles for CD4⁺ T cells in immunity to viruses. *Nat. Rev. Immunol.* **12**, 136–148 (2012).
44. Bollard, C. M. & Heslop, H. E. T cells for viral infections after allogeneic hematopoietic stem cell transplant. *Blood* **127**, 3331–3340 (2016).
45. Vasileiou, S. et al. Allogeneic, off-the-shelf, SARS-CoV-2-specific T cells (ALVR109) for the treatment of COVID-19 in high-risk patients. *Haematologica* **108**, 1840–1850 (2023).
46. Cruz, C. R. et al. Adverse events following infusion of T cells for adoptive immunotherapy: a 10-year experience. *Cytotherapy* **12**, 743–749 (2010).
47. Papadopoulou, A. et al. Systemic inflammatory response syndrome after administration of unmodified T lymphocytes. *Mol. Ther.* **22**, 1134–1138 (2014).
48. Bates, T. A. et al. Vaccination before or after SARS-CoV-2 infection leads to robust humoral response and antibodies that effectively neutralize variants. *Sci. Immunol.* **7**, eabn8014 (2022).
49. Rodda, L. B. et al. Imprinted SARS-CoV-2-specific memory lymphocytes define hybrid immunity. *Cell* **185**, 1588–1601 (2022).

50. Leen, A. M. et al. Multicenter study of banked third-party virus-specific T cells to treat severe viral infections after hematopoietic stem cell transplantation. *Blood* **121**, 5113–5123 (2013).
51. Service, R. F. Bad news for Paxlovid? Resistance may be coming. *Science* **377**, 138–139 (2022).
52. Iketani, S. et al. Multiple pathways for SARS-CoV-2 resistance to nirmatrelvir. *Nature* **613**, 558–564 (2023).
53. Rubin, R. From positive to negative to positive again—the mystery of why COVID-19 rebounds in some patients who take Paxlovid. *JAMA* **327**, 2380–2382 (2022).

Publisher's note Springer Nature remains neutral with regard to jurisdictional claims in published maps and institutional affiliations.

Springer Nature or its licensor (e.g. a society or other partner) holds exclusive rights to this article under a publishing agreement with the author(s) or other rightsholder(s); author self-archiving of the accepted manuscript version of this article is solely governed by the terms of such publishing agreement and applicable law.

© The Author(s), under exclusive licence to Springer Nature America, Inc. 2023

Anastasia Papadopoulou¹, **George Karavalakis**^{1,17}, **Efthymia Papadopoulou**^{2,17}, **Aliki Xochelli**³, **Zoi Bousiou**¹, **Anastasios Vogiatzoglou**², **Penelope-Georgia Papayanni**^{1,4}, **Aphrodite Georgakopoulou**^{1,4}, **Maria Giannaki**¹, **Fani Stavridou**¹, **Ioanna Vallianou**¹, **Maria Kammenou**¹, **Evangelia Varsamoudi**¹, **Vasiliki Papadimitriou**¹, **Chrysavgi Giannaki**⁵, **Maria Sileli**⁶, **Zoi Stergiouda**⁷, **Garyfallia Stefanou**⁸, **Georgia Kourlaba**⁹, **George Gounelas**⁸, **Maria Triantafyllidou**¹, **Eleni Siotou**¹, **Antonia Karaglani**¹⁰, **Eleni Zotou**^{1,4}, **Georgia Chatzika**³, **Anna Boukla**³, **Apostolia Papalexandri**¹, **Maria-Georgia Koutra**¹, **Dimitra Apostolou**¹¹✉, **Georgia Pitsiou**¹¹, **Petros Morfesis**¹², **Michalis Doulas**¹³, **Theodoros Karampatakis**¹⁴, **Nikolaos Kapravelos**⁵, **Militsa Bitzani**⁵, **Maria Theodorakopoulou**¹⁵, **Eva Serasli**², **Grigorios Georgolopoulos**¹, **Ioanna Sakellari**¹, **Asimina Fylaktou**³, **Stavros Tryfon**², **Achilles Anagnostopoulos**¹ & **Evangelia Yannaki**^{1,16}✉

¹Hematopoietic Cell Transplantation Unit, Department of Hematology Gene and Cell Therapy Center, George Papanikolaou Hospital, Thessaloniki, Greece. ²Department of Respiratory Medicine, George Papanikolaou Hospital, Thessaloniki, Greece. ³Department of Immunology, National Peripheral Histocompatibility Center, Hippokraton General Hospital, Thessaloniki, Greece. ⁴Department of Genetics, Development and Molecular Biology, School of Biology, Aristotle University of Thessaloniki, Thessaloniki, Greece. ⁵'A' Intensive Care Unit, George Papanikolaou Hospital, Thessaloniki, Greece. ⁶'B' Intensive Care Unit, George Papanikolaou Hospital, Thessaloniki, Greece. ⁷Department of Anesthesiology, George Papanikolaou Hospital, Thessaloniki, Greece. ⁸ECONCARE LP, Athens, Greece. ⁹Department of Nursing, University of Peloponnese, Tripolis, Greece. ¹⁰Euromedica Arogi Rehabilitation Center, Thessaloniki, Greece. ¹¹Department of Respiratory Failure, George Papanikolaou Hospital, Aristotle University of Thessaloniki, Thessaloniki, Greece. ¹²1st Department of Internal Medicine, AHEPA University Hospital, Aristotle University of Thessaloniki, Thessaloniki, Greece. ¹³2nd Propedeutic Department of Internal Medicine, Hippokrateio Hospital, Aristotle University of Thessaloniki, Thessaloniki, Greece. ¹⁴Department of Microbiology, George Papanikolaou Hospital, Thessaloniki, Greece. ¹⁵National and Kapodistrian University of Athens, Evaggelismos General Hospital, Athens, Greece. ¹⁶Department of Medicine, University of Washington, Seattle, WA, USA. ¹⁷These authors contributed equally: George Karavalakis, Efthymia Papadopoulou.
✉ e-mail: apostoloud8@gmail.com; eyannaki@u.washington.edu

Methods

Ethics

This study was conducted in accordance with the Declaration of Helsinki. Approval was obtained from the National Organization for Medicines and jurisdictional ethics committees (the National Ethics Committee (NEC) and the institutional review boards of George Papanikolaou Hospital and Hippokrateion Hospital) after thorough discussions and protocol adjustments on eligibility criteria and safety assessments and an interim and final review of the phase 1 study data (NEC) before beginning the phase 2 study. A continuous safety surveillance by pharmacovigilance was also integrated into all study phases. All patients provided written informed consent. EudraCT identifier: [2021-001022-22](https://www.eudract.eu/number/2021-001022-22); ClinicalTrials.gov identifier: [NCT05447013](https://www.clinicaltrials.gov/ct2/show/study/NCT05447013).

Trial design

This was a randomized 2:1, open-label, phase 1/2 trial, conducted between June 2021 and February 2022 (first and last patients were enrolled on 2 June 2021 and 7 December 2021, respectively), when the Delta variant predominated. The study evaluated the safety and efficacy of CoV-2-STs+SoC compared to SoC in hospitalized adults with severe COVID-19. All patients in both arms received SoC, which included remdesivir, low-molecular-weight heparin, dexamethasone (6 mg per day for 5 d), azithromycin, oxygen supply and, as necessary, ICU support. Inclusion criteria were as follows: (1) molecularly confirmed COVID-19; (2) symptom onset within 6 d; (3) pneumonia or oxygen saturation on air $\leq 94\%$; (4) $CD3^+$ cells ≤ 650 per microliter; and (5) at least one increased biomarker (CRP ($\geq 3\times$ the upper limit of normal (ULN)), LDH ($\geq 2\times$ ULN), ferritin ($>1,000$ ng ml $^{-1}$), D-dimers ($\geq 2\times$ ULN)) and age ≥ 18 years or ≤ 80 years. Main exclusion criteria involved the administration of corticosteroids at a dose of >0.75 mg kg $^{-1}$ (methylprednisolone equivalent), the presence of ARDS and multi-organ failure, mechanical ventilation and KS < 50 . Detailed eligibility criteria are provided in Supplementary Table 8.

In a '3 + 3' design⁵⁴ phase 1 study, two escalated cell doses were assessed. For the next phase of the study, a sample size of 90 male or female participants was deemed adequate for a phase 2 trial—that is, 10–15% of the total sample size estimated (13%), by assuming a 2:1 allocation, a recovery rate of 1.30 within 30 d, 5% for type I error and 90% for power.

Eligible participants were randomly assigned (2:1) to receive either CoV-2-STs and SoC (CoV-2-STs+SoC group, arm A) or SoC alone (SoC group, arm B) and followed for 60 d. The randomization sequence was generated in RStudio using the binomial distribution by an independent statistician, and it remained concealed from the study investigators; for each codified entrance in the study, the assigned treatment was revealed to investigators by telephone.

CoV-2-ST products were selected based on the presence of at least either one common with the recipient HLA mediating viral specificity or two common HLAs, by prioritizing matching at HLA-DRB1 when possible, given that the CoV-2-ST cell products were dominated by CD4 $^+$ cells. HLA typing was conducted with priority, and the cells were administered within a maximum of 24 h after randomization (day 0 for both arms; Supplementary Fig. 12). All data for eligible participants were collected at George Papanikolaou Hospital and Hippokrateion Hospital at pre-specified time-points. No major protocol deviations occurred; three participants initially signed a previous version of the consent form and were subsequently re-consented by signing the correct version. Four patients missed their visits within the permitted timeframe, and one was lost to follow-up. After the completion of the enrollment and treatment of the 90 patients presented here, the trial was amended to include additional patients and is still open. The corresponding version of the study protocol is available as a supplement to the full text of this article (Appendix B).

CoV-2-ST donors

CoV-2-ST donors comprised 30 (of 70 evaluated) healthcare professionals, aged ≤ 58 years, who recovered from wild-type COVID-19, had

no serious underlying disease, developed strong SARS-CoV-2-specific T cell immunity and expressed the most frequent HLA molecules in the Greek population (as determined by reviewing the HLA database of HSCT recipients at our center). In 18 convalescent donors, vaccination had preceded donation (Supplementary Table 1). All donors provided written informed consent.

CoV-2-ST generation

CoV-2-STs were generated under GMP standards using 35–45 ml of donor blood. PBMCs were pulsed with 0.5 $\mu\text{g ml}^{-1}$ spike, membrane and NCAP 15mer, overlapping pepmixes (customized pepmixes, JPT Peptide Technologies) and cultured for 9–11 d in G-Rex10 (80040S, Wilson Wolf Manufacturing) with 10 ng ml $^{-1}$ IL-7 (207-GMP, R&D Systems) and 400 U ml $^{-1}$ IL-4 (204-GMP, R&D Systems)^{7,8,21,55}. The generated cell products were stored in liquid nitrogen to be used off the shelf in a subsequent phase 1/2 trial.

Assessments

Patients were assessed daily from day 0 for the eight-category OS score (Supplementary Table 9), safety, discharge, intubation or death. Clinical data were recorded on paper case record forms and then entered into an electronic database. Laboratory assessments were performed on days 3, 5 (± 2), 10 (± 2), 15 ($+3$), 22 ($+3$), 30 ($+3$), 45 ($+3$) and 60 ($+7$) and additionally as indicated. AEs were assessed through the end of study participation (60 d after enrollment).

Outcome measurements

Major safety endpoints were any acute toxicity associated with the cell therapy, the development of CRS and the rates of AEs and SAEs in either arm. To differentially diagnose a CRS in the form of ARDS associated with hyperinflammatory COVID-19 from a rare, but possible, CoV-2-ST-induced CRS, we were based on the more profound cytokine (especially IL-6) or acute-phase reactant elevations (especially ferritin) observed in T-cell-induced CRS (than COVID-19 ARDS) and the greater elevations of D-dimers found in hyperinflammatory COVID-19 (than T-cell induced CRS) (Supplementary Table 4)²⁴. Secondary endpoint was the development of GvHD. Toxicities were graded according to National Cancer Institute Common Toxicity Criteria of Adverse Events (version 4.03). Toxicities and AEs were analyzed in the treated population. Primary efficacy endpoints were (1) the composite endpoint of time to recovery (defined as the first day after randomization (day 0) on which a patient scored ≤ 3 in the eight-category OS (Supplementary Table 9)), recovery rate ratio and the percentage of recovered patients and (2) the in vivo expansion of CoV-2-STs. The key secondary outcome was day 60 survival. Other secondary outcomes included the time to polymerase chain reaction (PCR) negativity, time to lymphopenia recovery, hospitalization length, intubation/extubation incidence and the in vivo persistence of donor CoV-2-STs.

Viral load

SARS-CoV-2 viral load from nasopharyngeal samples was assessed by real-time PCR using commercially available kits (Fast PCR Detection Kit version 5.1, 3103010069, 3D Biomedicine Science & Technology Co., Ltd.) as per the manufacturer's instructions. To quantitate viral RNA, a standard curve was obtained by amplification of known amounts of SARS-CoV-2 RNA (3D Med Verification Kit 2, 3000000000038, 3D Biomedicine Science & Technology Co., Ltd.). Four consecutive dilutions were prepared from 24,000 to 400 copies per milliliter. The amounts of SARS-CoV-2 RNA in patient samples were obtained by plotting cycle threshold (Ct) values onto the standard curve against the log of the standard sample amount. After discharge from the hospital, for some patients the SARS-CoV-2 negativation was assessed by the rapid diagnostic test.

CoV-2 Nabs

CoV-2 Nabs were measured in serum by a competitive chemiluminescence immunoassay on the Snibe Maglumi 800 analyzer (Maglumi SARS-CoV-2

Neutralizing Antibody CLIA, 130219027M, Snibe Diagnostic). CoV-2 Nabs compete with the angiotensin-converting enzyme 2 antigen immobilized on a solid phase for binding to labeled SARS-CoV-2 spike receptor-binding domain, producing a light signal that is inversely proportional to the sample CoV-2 Nabs. CoV-2 Nabs $\geq 0.3 \mu\text{g ml}^{-1}$ were regarded as positive.

ELISpot assay

PBMCs or T cell products were pulsed with a mix peptide pool of spike, membrane and NCAP antigens (PM-WCPV-S-1 or 2, PM-WCPV-NCAP-1 and PM-WCPV-VME-2, JPT Peptide Technologies) or spike only (unmutated, Alpha, Beta, Delta or Omicron variant of spike; PM-SARS2-SMUT01-1, PM-SARS2-SMUT02-1, PM-SARS2-SMUT06-1 and PM-SARS2-SMUT08-1, JPT Peptide Technologies) or individual or pooled SARS-CoV-2 epitopes known to be restricted through specific HLAs (customized peptides, JPT Peptide Technologies) (Supplementary Table 10). Specificity was measured by ELISpot (Eli.Scan scanner (A.EL.VIS), Eli.Analyse software V6.2.SFC) as IFN- γ -secreting cells and expressed as SFCs per number of input cells (3420-2AST-2, Mabtech). Response was considered positive if the total cytokine-producing SFCs against antigens tested were ≥ 30 per 5×10^3 PBMCs or 2×10^5 CoV-2-STs.

Flow cytometry

Samples were acquired on a FACSCalibur device (Becton Dickinson). All analyses were performed with CellQuest Pro 6 software or FlowJo version 10. Gating strategies are illustrated in Supplementary Figs. 13–15.

Absolute cell numbers. Peripheral blood cells were stained with CD45 APC (clone 2D1, 340910, BD Biosciences, dilution 1:20), CD3 FITC (clone UCHT1, 1F-514-T100, EXBIO, dilution 1:5), CD4 PE-Cyanine5 (clone RPA-T4, CYT-4C1, Cytognos, dilution 1:20) and CD56 PE (clone C5.9, CYT-56PE, Cytognos, dilution 1:20), and the absolute number of lymphocyte subpopulations per microliter of blood was analyzed with BD TruCount technology.

Immunophenotyping. CoV-2-STs were stained with CD3 APC (clone SK7, 345767, BD Biosciences, dilution 1:20), CD8 PE (clone MEM-31, 1P-207-T100, EXBIO, dilution 1:5), CD45RA PE (clone MEM-56, 1P-223-T100, EXBIO, dilution 1:5) and CD62L APC (clone LT-TD180, 1A-449-T100, EXBIO, dilution 1:10). T cell subsets were defined as follows: naive; CD3⁺CD45RA⁺CD62L⁺, EM; CD3⁺CD45RA⁺CD62L⁻, CM; CD3⁺CD45RA⁻CD62L⁺ and TEMRA; and CD3⁺CD45RA⁻CD62L⁻.

Cytokine evaluation. Serum cytokine measurements were performed by using a multiplex cytokine assay (AimPlex Biosciences, C191051) as per the manufacturer's instructions.

HLA typing

DNA samples from CoV-2-ST donors were typed for HLA-A*, -B*, -C*, -DRB1*, -DRB3*, -DRB4*, -DRB5*, -DQA1*, -DQB1*, -DPA1* and -DPB1*. High-resolution 2F typing was performed either by PCR-SSP using PCR amplification with sequence-specific primers (SSPRI-24, SSPRI-33, SSPRI-05, SSPRI-21, SSPRI-40, SSPRI-2-111, SSPRI-2-113, SSPRI-2-116, SSPRI-2LQBI, Micro SSP; One Lambda) or by next-generation sequencing (NGS). NGS-based HLA typing was performed using the AllType FASTplex kit (ALL-FAST11LX, One Lambda) for library preparation, Ion Chef for chip preparation (IONCHEF-EXT, One Lambda) and Ion GeneStudio S5 (IONS5-530C4, Thermo Fisher Scientific) for sequencing.

All patients were typed for HLA-A, -B and -DRB1. Low-resolution typing was performed either by PCR-SSP (PROTRANS Cyclerplate System HLA A*-B*-DRB1* REF 020,200, Morgan HLA A SSP 33240, HLA DRB SSP 33280, TBG Biotechnology Corp., inno-train Diagnostik HLA-Ready Gene HLA B 002051020) or by PCR-SSO (using PCR amplification and subsequent hybridization with sequence-specific

oligonucleotide probes (RSSO1B, LABType SSO Luminex/One Lambda Kit, LIFE CODES HLA-A 628911, HLA-DRB1 628923, SSO Typing Kits, IMMUCOR)).

Genomic analysis

Quantitative determination of donor's lymphocytes compared to recipient in sequential samples was based on chimerism level of donor's DNA compared to total DNA measured by NGS. Due to inadequate numbers of patient PBMCs, mainly at the early stage of lymphopenia, and to obtain measurable cell representation in patient samples, PBMCs were pulsed with CoV-2-ST pepmixes and ex vivo expanded before the assay. Genomic DNA was isolated from T lymphocytes using the QIAamp Mini DNA Kit (51104, Qiagen). Chimerism level was quantified using the Devyser Chimerism kit (8-A107), based on targeted sequencing of 24 indels for screening of a recipient/donor pair and measuring their allele frequency. A total of 60 ng of genomic DNA was used to build the libraries, quantified by Qubit (Thermo Fisher Scientific) and sequenced on a MiniSeq System in a 2×150 -bp run (Illumina). Sequences were analyzed using Advyser for Chimerism software version 3.0.1.0 where coverage of more than 10,000 reads is required to determine chimerism at 0.1% sensitivity.

Analysis plan and statistical methodology

Sample size calculation. Our study was powered only for the composite primary endpoint of time to recovery and day 30 proportion of recovered patients without considering the co-primary endpoint of the expansion of CoV-2-STs over time, as, at that time, there were no pre-existing data on the effect size for CoV-2-ST expansion in patients with COVID-19. We assumed a recovery ratio equal to 1.35 used in the remdesivir ACTT-1 trial study (including patients with moderate to severe COVID-19) (ref. 6), a 2:1 ratio between the two compared groups (CoV-2-STs+SoC versus SoC), $\alpha = 0.05$ and power 90%, and we adjusted the final sample size between 10% and 15% of the calculated (90 (60/30) from 656 (440/216)), considering this phase 1/2 study as a 'pilot' of a phase 3 confirmatory study, for which a subset of the final sample size (3–5%) (ref. 56) could be considered satisfactory.

Primary analysis according to pre-specified analysis plan. Differences in baseline characteristics between the two arms were assessed by Student's *t*-test or Mann-Whitney *U*-test after testing for normality with the Shapiro-Wilk test (continuous variables were expressed as needed with mean and s.d. or median and 1st–3rd quartiles) and Pearson's chi-square or Fisher's exact test (categorical variables were expressed as absolute (*n*) and relative (%) frequencies). Time-to-event analyses were performed using Kaplan-Meier curves stratified by treatment group, log-rank test to assess the difference between groups and Cox model for the estimation of HR and 95% CIs. RRs with 95% CIs for mortality and recovery endpoints were determined by the Mantel-Haenszel method, with treatment comparison assessed with a logistic regression model. A stratified analysis was performed for day 30 recovery and day 60 mortality for age categories, gender, KS and vaccination status. KS was selected among other disease severity variables, as all were highly correlated (KS, oxygen supply and OS). All analyses of treatment effect (STATA version 17) used mITT (main analysis) and an AT approach (Fig. 1), with endpoints being analyzed at a 0.05 significance level (two-sided). No adjustments for multiplicity were made in the analysis of secondary outcomes, including survival; thus, they should be considered descriptive and not used to infer treatment effects.

Longitudinal data analysis. All longitudinal data on immunological responses, including immune cell populations, CoV-2-ST expansion and Nab kinetics in response to arm, vaccination or survival status, were analyzed by applying linear regression and correction for multiple comparisons where indicated. Model selection was performed

by backward elimination using the likelihood ratio test (R package *lmtest*) and a chi-square P value cutoff of 0.05, starting with interaction between arm and vaccination. Days after enrollment was fitted as a quadratic term except for NK kinetics. Response variables were log-transformed except for CoV-2-NAb counts, which were normalized by ordered quantile normalization (R package *bestNormalize*). Post hoc analysis between groups was performed using the Tukey HSD test using the *mosaic* R package, with correction for multiple comparisons where applicable and significance cutoff of $P < 0.05$. All analyses and visualizations were performed in R version 4.2.2. Differences between datasets on specificity of CoV-2-ST products or day 10 circulating CoV-2-STs were analyzed using one-way ANOVA with false discovery rate (FDR) multiple testing corrections using the two-stage step-up method from Benjamini, Krieger and Yekutieli ($P < 0.05$ and $q < 0.05$) or a Mann–Whitney test or a two-tailed Student's t -test for two-group comparisons (GraphPad Prism).

Reporting summary

Further information on research design is available in the Nature Portfolio Reporting Summary linked to this article.

Data availability

George Papanikolaou Hospital is committed to responsible and transparent sharing of clinical trial data with healthcare practitioners and researchers, toward the improvement of scientific knowledge and the promotion of innovative medical approaches. Participant de-identified data collected for this study, including text, tables, figures, appendices and documents, including the study protocol, statistical analysis plan and informed consent form, will be available after article publication. Researchers interested in obtaining access to documents and/or data for academic use only can make their request by submitting the scientific design, specific data needs and analysis and dissemination plans, which will be reviewed by the institutional review board of George Papanikolaou Hospital, and, based on scientific merit, data access could be granted. An agreement will be signed between the two parties stating that the data will be used only for the agreed purpose, in compliance with ethical and regulatory requirements and the commitments made to the study participants. Any publication derived from the accessed data should be of high quality, and George Papanikolaou Hospital's institutional review board will have the right to review and comment on any draft manuscripts before publication.

References

54. US Food and Drug Administration. Clinical Considerations for Therapeutic Cancer Vaccines: Guidance for Industry. <https://www.fda.gov/regulatory-information/search-fda-guidance-documents/clinical-considerations-therapeutic-cancer-vaccines> (2011).
55. Papadopoulou, A. et al. Clinical-scale production of *Aspergillus*-specific T cells for the treatment of invasive aspergillosis in the immunocompromised host. *Bone Marrow Transpl.* **54**, 1963–1972 (2019).
56. Stallard, N. Optimal sample sizes for phase II clinical trials and pilot studies. *Stat. Med.* **31**, 1031–1042 (2012).

Acknowledgements

We express our sincere thanks to the donors and patients. We thank all healthcare professionals who took care of the patients on hard times. This work was supported by the Committee of 'Greece 2021' and George Papanikolaou Hospital. We also greatly appreciate the support of community fundraising. The funders had no role in study design, data collection and analysis, decision to publish or preparation of the manuscript.

Author contributions

Study design and development of concept: A.P. and E.Y. GMP production and quality assurance: A.P., P.-G.P., A.G., I.V. and E.Y. Patient management: G.K., E.P., Z.B., M.K., E.V., V.P., A.V., E. Serasli, I.S., A.A., S.T., M.S., Z.S., N.K., M.B., M.T., D.A., G.P., M.D. and E.Y. Data collection: E.P., Z.B., A.V., M.G., F.S., A.X., A.F., P.-G.P., A.G., I.V., M.T., M.D., P.M., T.K., G.C., A.B., A.P. and M.G.K. Data analysis: G.S., G.K., G. Gounelas, G. Georgolopoulos, A.P. and E.Y. Study coordination: E.Y. and A.P. Obtained funding: E.Y. and A.A. Wrote the manuscript: A.P. and E.Y. All authors reviewed and revised the final manuscript.

Competing interests

The authors declare no competing interests.

Additional information

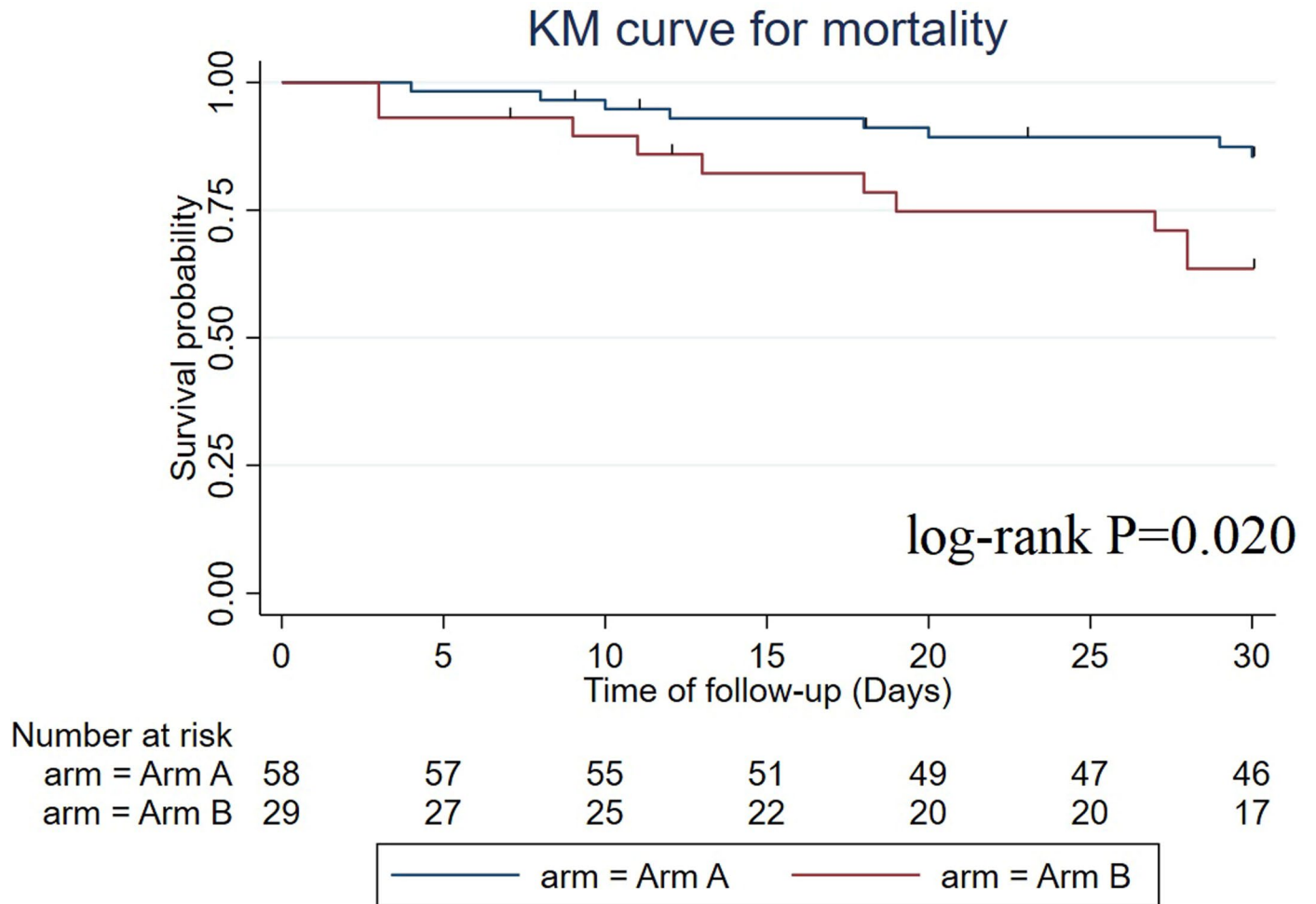
Extended data is available for this paper at <https://doi.org/10.1038/s41591-023-02480-8>.

Supplementary information The online version contains supplementary material available at <https://doi.org/10.1038/s41591-023-02480-8>.

Correspondence and requests for materials should be addressed to Dimitra Apostolou or Evangelia Yannaki.

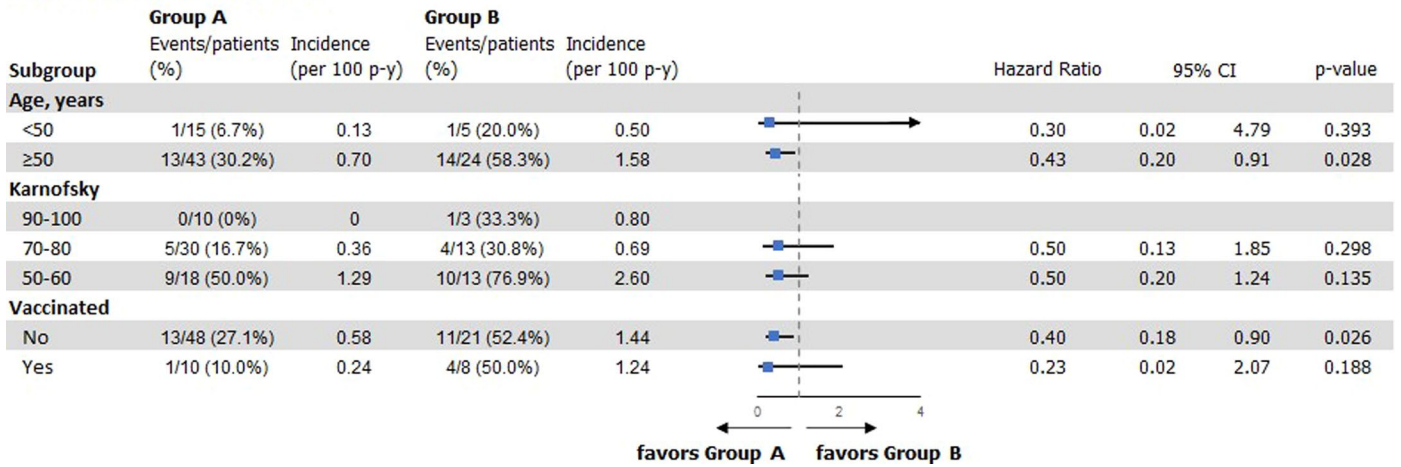
Peer review information *Nature Medicine* thanks Cliona Rooney, Katherine Kedzierska and Michael Schell for their contribution to the peer review of this work. Primary handling editor: Alison Farrell, in collaboration with the *Nature Medicine* team.

Reprints and permissions information is available at www.nature.com/reprints.

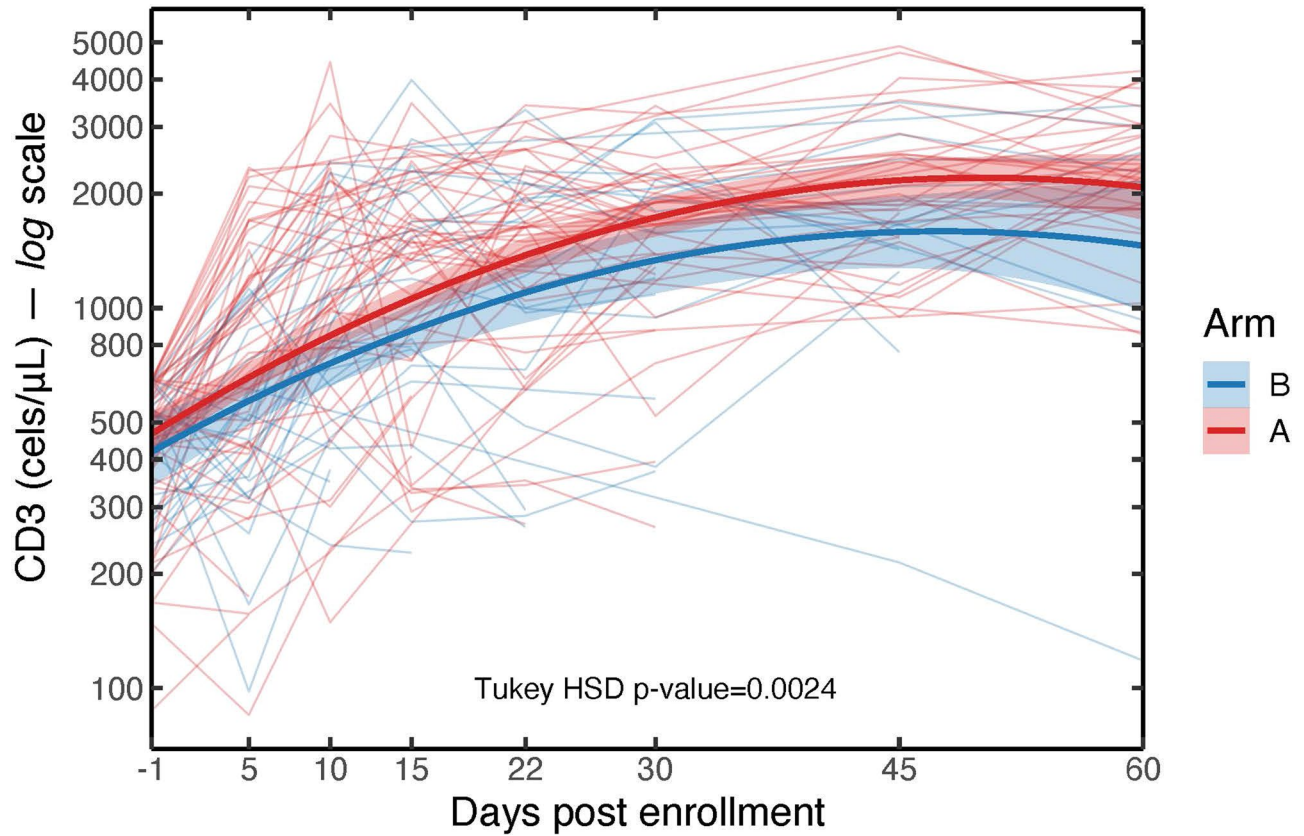


Extended Data Fig. 1 | Kaplan-Meier curves for mortality (time to death) at 30 days in the modified intention-to-treat (mITT) population. P value was calculated using the two-sided log-rank test.

Mortality at 60 days - mITT population

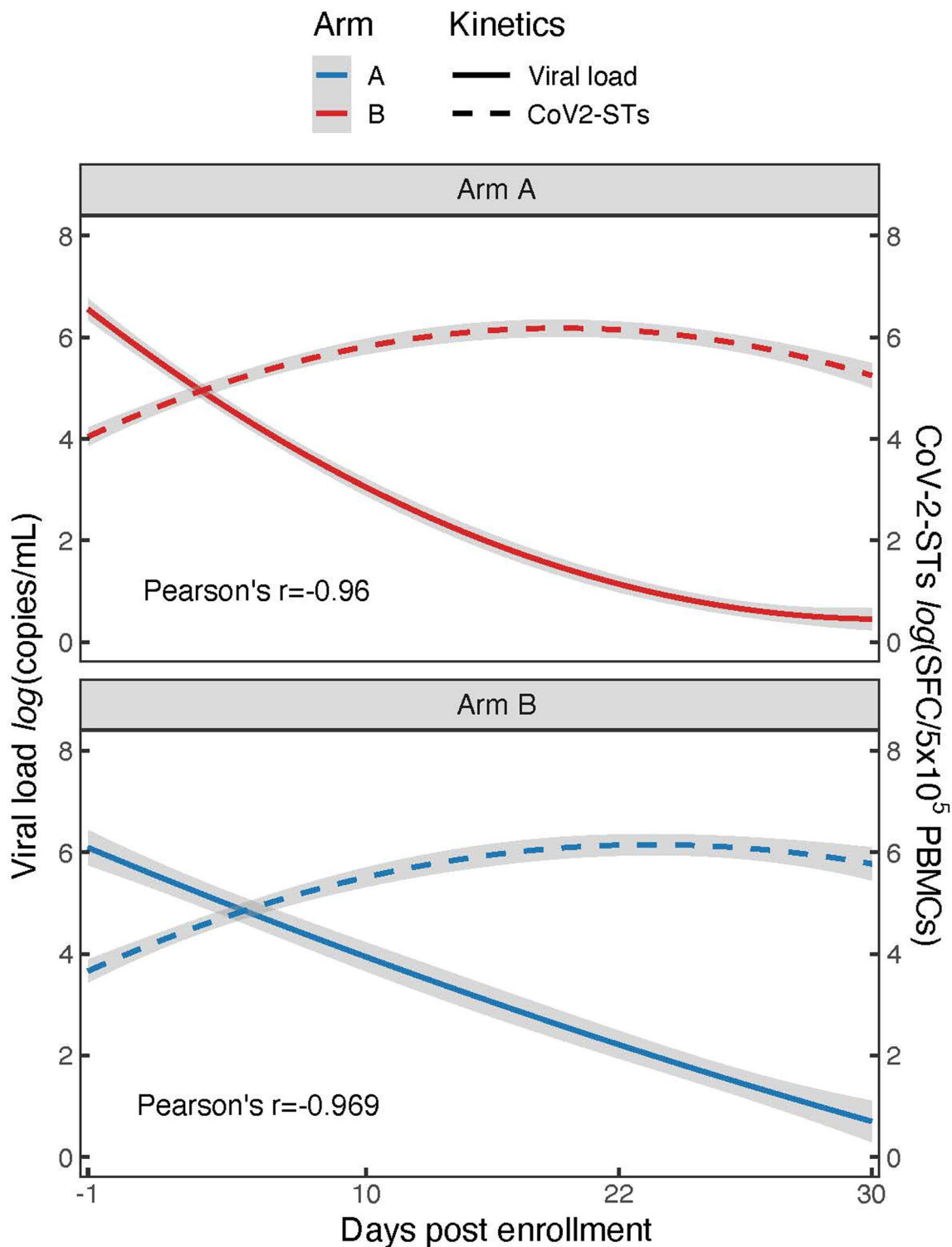


Extended Data Fig. 2 | Subgroup analysis on mortality at 60 days, in the and mITT population. mITT: modified intention-to-treat analysis. Two-sided Wald test-based P values (as calculated using Cox regression). All P values shown are unadjusted for multiple testing and should therefore not be used to infer treatment effects.



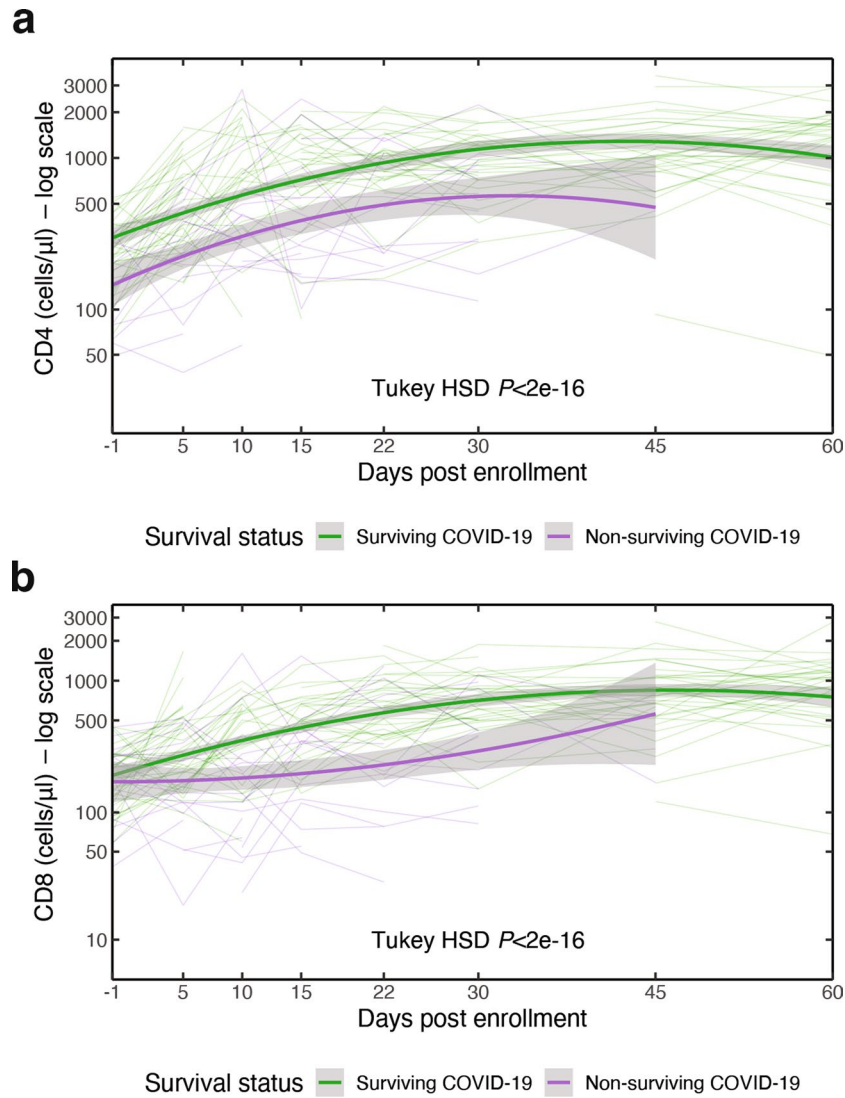
Extended Data Fig. 3 | Longitudinal analysis of T lymphocyte recovery kinetics over the study period in CoV-2-ST+SoC-treated (red lines, n = 58) and SoC-treated (blue lines, n = 29) patients. The thin lines represent

individual CD3+ cell values for each patient. Bold lines are the quadratic fitted splines for each group. Shaded bands extend to 95% CI of the fitted values. Tukey HSD p-value is reported.



Extended Data Fig. 4 | Correlation of the kinetics of circulating CoV-2-STs and viral load, in CoV-2-STs+SoC-treated (n = 57) and SoC-treated (n = 30) patients. The dotted lines represent the fitted values of circulating CoV-2-STs,

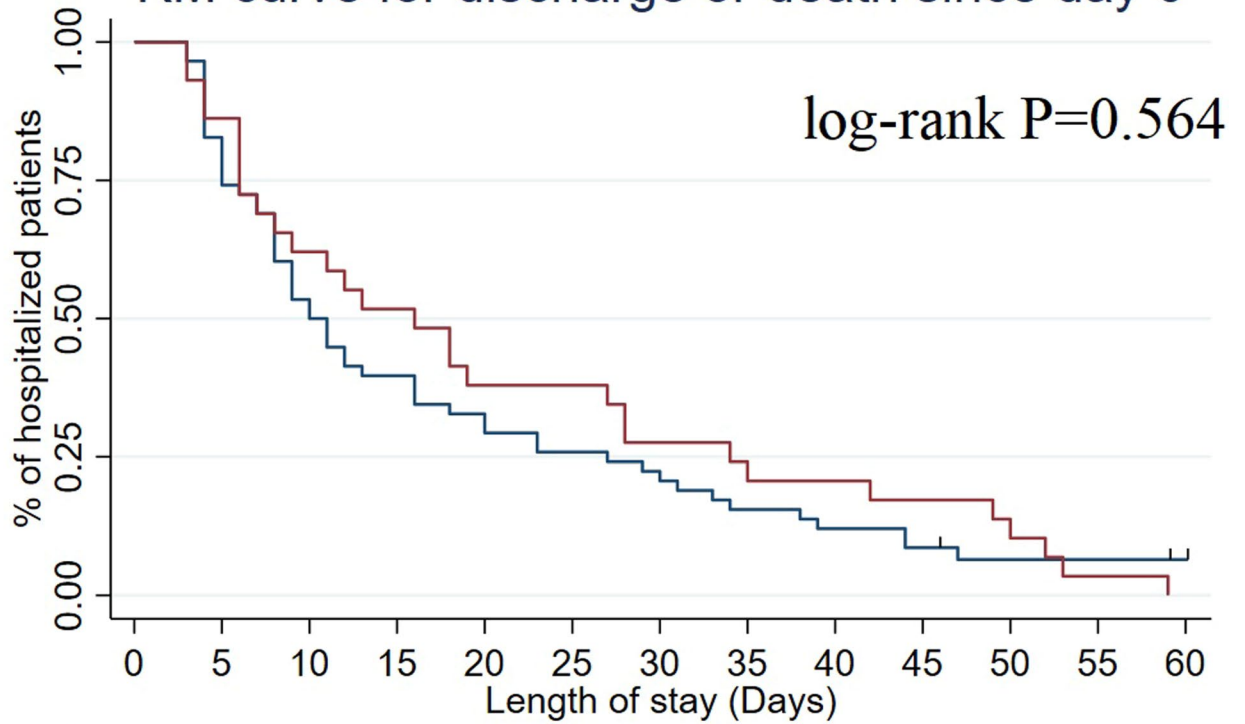
the solid lines represent the fitted values of SARS-CoV-2 viral load. Shaded bands extend to 95% CI of fitted values. Pearson's correlation coefficient values are reported.



Extended Data Fig. 5 | Longitudinal trajectories of circulating CD4 (A) and CD8+ (B) cells in surviving (green lines, n = 58) and non-surviving (purple lines, n = 29) COVID-19 patients. Thin lines represent individual cell population

counts for each patient. Bold lines are the quadratic fitted splines of each group. Shaded bands represent the 95% CI of the fitted values. One-way ANOVA p-values are reported for the survival status effect on both CD4 and CD8 trajectories.

KM curve for discharge or death since day 0



Number at risk

arm = Arm A	58	48	31	23	19	15	13	9	7	5	3	3	1
arm = Arm B	29	25	18	15	11	11	8	7	6	5	4	1	0



Extended Data Fig. 6 | Kaplan-Meier curve for hospitalization length at 60 days in the MITT population. P value was calculated using the two-sided log-rank test.

Extended Data Table 1 | Safety information

Extended Data Table 1. Safety information									
	Any Grade			Grade 3-4			Grade 5		
	CoV-2-STs + SoC (N=57)	SoC (N=30)	p-value	CoV-2-STs + SoC (N=57)	SoC (N=30)	p-value	CoV-2-STs + SoC (N=57)	SoC (N=30)	p-value
Any adverse event									
Anemia	21 (36.8%)	11 (36.7%)	0.987 ⁺	7 (12.3%)	5 (16.7%)	0.573	0 (0.0%)	0 (0.0%)	-
Neutropenia	2 (3.5%)	0 (0.0%)	0.543‡	1 (1.8%)	0 (0.0%)	> 0.999‡	0 (0.0%)	0 (0.0%)	-
Platelets<100.000	9 (15.8%)	6 (20%)	0.621 ⁺	4 (7%)	2 (6.7%)	> 0.999‡	0 (0.0%)	0 (0.0%)	-
INR>1.5	2 (3.5%)	5 (16.7%)	0.045‡	0 (0.0%)	1 (3.3%)	0.345‡	0 (0.0%)	0 (0.0%)	-
Increased Aspartate aminotransferase	19 (33.3%)	12 (40%)	0.537 ⁺	1 (1.8%)	0 (0.0%)	> 0.999‡	0 (0.0%)	0 (0.0%)	-
Increased Alanine aminotransferase	20 (35.1%)	12 (40%)	0.652 ⁺	1 (1.8%)	0 (0.0%)	> 0.999‡	0 (0.0%)	0 (0.0%)	-
Increased bilirubin	1 (1.8%)	2 (6.7%)	0.272‡	0 (0.0%)	1 (3.3%)	0.345‡	0 (0.0%)	0 (0.0%)	-
Increased creatinine	3 (5.3%)	4 (13.3%)	0.228‡	1 (1.8%)	1 (3.3%)	> 0.999‡	0 (0.0%)	0 (0.0%)	-
Hyperamylasaimia	0 (0.0%)	1 (3.3%)	0.345‡	0 (0.0%)	1 (3.3%)	0.345‡	0 (0.0%)	0 (0.0%)	-
Hypoalbuminemia	23 (40.4%)	13 (43.3%)	0.788 ⁺	1 (1.8%)	2 (6.7%)	0.272‡	0 (0.0%)	0 (0.0%)	-
Chest pain	0 (0.0%)	0 (0.0%)	-	0 (0.0%)	0 (0.0%)	-	0 (0.0%)	0 (0.0%)	-
Epistaxis	1 (1.8%)	0 (0.0%)	> 0.999‡	0 (0.0%)	0 (0.0%)	-	0 (0.0%)	0 (0.0%)	-
Hepatitis B reactivation	1 (1.8%)	0 (0.0%)	> 0.999‡	0 (0.0%)	0 (0.0%)	-	0 (0.0%)	0 (0.0%)	-
Hemolysis	1 (1.8%)	0 (0.0%)	> 0.999‡	0 (0.0%)	0 (0.0%)	-	0 (0.0%)	0 (0.0%)	-
Dyspepsia	0 (0.0%)	1 (3.3%)	0.345‡	0 (0.0%)	1 (3.3%)	0.345‡	0 (0.0%)	0 (0.0%)	-
Diarrhea	2 (3.5%)	1 (3.3%)	> 0.999‡	1 (1.8%)	1 (3.3%)	> 0.999‡	0 (0.0%)	0 (0.0%)	-
Superficial thrombophlebitis	0 (0.0%)	1 (3.3%)	0.345‡	0 (0.0%)	0 (0.0%)	-	0 (0.0%)	0 (0.0%)	-
Skin rash	1 (1.8%)	0 (0.0%)	> 0.999‡	0 (0.0%)	0 (0.0%)	-	0 (0.0%)	0 (0.0%)	-
Sinus bradycardia	1 (1.8%)	0 (0.0%)	> 0.999‡	0 (0.0%)	0 (0.0%)	-	0 (0.0%)	0 (0.0%)	-
Serious adverse event									
ARDS/Acute respiratory failure	19 (33.3%)	15 (50.0%)	0.130 ⁺	7 (12.3%)	3 (10%)	0.710‡	12 (21.1%)	12 (40%)	0.053 ⁺
Sepsis	11 (19.3%)	11 (36.7%)	0.076 ⁺	4 (7%)	2 (6.7%)	> 0.999‡	7 (12.3%)	9 (30%)	0.043⁺
Thromboembolic event	2 (3.5%)	2 (6.7%)	0.606‡	1 (1.8%)	1 (3.3%)	> 0.999‡	1 (1.8%)	1 (3.3%)	> 0.999‡
Acute kidney injury	1 (1.8%)	2 (6.7%)	0.272‡	1 (1.8%)	1 (3.3%)	> 0.999‡	0 (0.0%)	1 (3.3%)	0.345‡
Cardiac arrest	2 (3.5%)	2 (6.7%)	0.606‡	0 (0.0%)	0 (0.0%)	-	2 (3.5%)	2 (6.7%)	0.606‡
Pneumothorax/Subcutaneous emphysema	4 (7.0%)	2 (6.7%)	> 0.999‡	2 (5.3%)	2 (6.7%)	0.603‡	1 (1.8%)	0 (0.0%)	> 0.999‡
Stroke	1 (1.8%)	0 (0.0%)	> 0.999‡	1 (1.8%)	0 (0.0%)	> 0.999‡	0 (0.0%)	0 (0.0%)	-
Pancreatic necrosis	0 (0.0%)	1 (3.3%)	0.345‡	0 (0.0%)	1 (3.3%)	0.345‡	0 (0.0%)	0 (0.0%)	-

+ Pearson's chi-square test; ‡ Fischer's exact test; Bold font indicates statistical significance. All statistical tests were two-sided.

Reporting Summary

Nature Portfolio wishes to improve the reproducibility of the work that we publish. This form provides structure for consistency and transparency in reporting. For further information on Nature Portfolio policies, see our [Editorial Policies](#) and the [Editorial Policy Checklist](#).

Statistics

For all statistical analyses, confirm that the following items are present in the figure legend, table legend, main text, or Methods section.

n/a | Confirmed

- The exact sample size (n) for each experimental group/condition, given as a discrete number and unit of measurement
- A statement on whether measurements were taken from distinct samples or whether the same sample was measured repeatedly
- The statistical test(s) used AND whether they are one- or two-sided
Only common tests should be described solely by name; describe more complex techniques in the Methods section.
- A description of all covariates tested
- A description of any assumptions or corrections, such as tests of normality and adjustment for multiple comparisons
- A full description of the statistical parameters including central tendency (e.g. means) or other basic estimates (e.g. regression coefficient) AND variation (e.g. standard deviation) or associated estimates of uncertainty (e.g. confidence intervals)
- For null hypothesis testing, the test statistic (e.g. F , t , r) with confidence intervals, effect sizes, degrees of freedom and P value noted
Give P values as exact values whenever suitable.
- For Bayesian analysis, information on the choice of priors and Markov chain Monte Carlo settings
- For hierarchical and complex designs, identification of the appropriate level for tests and full reporting of outcomes
- Estimates of effect sizes (e.g. Cohen's d , Pearson's r), indicating how they were calculated

Our web collection on [statistics for biologists](#) contains articles on many of the points above.

Software and code

Policy information about [availability of computer code](#)

Data collection Designated staff collected the data as specified in the protocol. Data were first collected in hard copy and then entered in the Electronic Case Report Form (eCRF), constructed using fully validated web-secured software.

Data analysis Statistical analysis was performed using STATA v.17 or R version 4.2.2 or GraphPad Prism v.7. All flow cytometry analyses were performed with the CellQuest Pro6 software or FlowJo V10. NGS sequences were analyzed using the ADVYSER for Chimerism software 3.0.1.0 version

For manuscripts utilizing custom algorithms or software that are central to the research but not yet described in published literature, software must be made available to editors and reviewers. We strongly encourage code deposition in a community repository (e.g. GitHub). See the Nature Portfolio [guidelines for submitting code & software](#) for further information.

Data

Policy information about [availability of data](#)

All manuscripts must include a [data availability statement](#). This statement should provide the following information, where applicable:

- Accession codes, unique identifiers, or web links for publicly available datasets
- A description of any restrictions on data availability
- For clinical datasets or third party data, please ensure that the statement adheres to our [policy](#)

George Papanikolaou Hospital is committed to responsible and transparent sharing of clinical trial data with healthcare practitioners and researchers for academic use only, towards the improvement of scientific knowledge and the promotion of innovative medical approaches and based on scientific merit. Participant de-

identified data (in line with applicable laws and regulations) collected for the study, including text, tables, figures, appendices as well as documents including the study protocol, statistical analysis plan, informed consent form, will be available following article publication. Researchers interested in obtaining access to documents and/or data for academic use only, can make their request submitting the scientific design, specific data needs, analysis and dissemination plans, which will be reviewed by the IRB of the George Papanikolaou Hospital and based on scientific merit, should data access could be granted. An agreement will be signed between the two parties stating that the data will only be used for the agreed purpose, in compliance to ethical and regulatory requirements and the commitments made to the study participants. Any publication derived from the accessed data should be of high quality and the George Papanikolaou Hospital's IRB will have the right to review and comment on any draft manuscripts before publication. The study data are not available in public databases as they contain information that could compromise participant's consent.

Human research participants

Policy information about [studies involving human research participants and Sex and Gender in Research](#).

Reporting on sex and gender

Only sex (self reported) was considered for demographic purposes. Both men and women were recruited for phase I and II of the trial, 54 men and 39 women). As commonly seen in severe COVID-19, more men than women were identified with severe disease and proved eligible.

Population characteristics

We screened 94 COVID-19 hospitalized patients for eligibility. Of these, 90 met the inclusion criteria and were randomly assigned (2:1) to either receiving CoV-2-STs+SoC (Arm-A) or SoC-only (Arm-B). Three patients withdrew consent and one patient, initially allocated to CoV-2-STs-cohort, was intubated prior to receiving the cells. A total of 87/90 randomized patients were included in the modified intention-to-treat (Arm-A:58; Arm-B:29) and as-treated analysis (Arm-A:57; Arm-B:30). In the total cohort, the median age was 57 years [interquartile range (IR) 50-67], 21% of the patients were vaccinated, 40% were female, 85% had a Karnofsky score between 50 and 80, 48% had high needs for oxygen supply due to severely impaired respiratory function and more than half had at least 2 comorbidities. The baseline demographic and disease characteristics were well balanced between the two groups, with only exception the incidence of diabetes, being higher in the SoC-arm. The median time from symptoms' onset or consent to day-0 was 5 and 2 days, respectively, in both arms. Population characteristics are shown in detail in Table 1.

Recruitment

To minimize selection bias, recruitment was based on objective pre-defined criteria of SARS-COV-2 positive PCR, symptoms onset within 6 days, hypoxemia/pneumonia and a specified increase of an inflammatory biomarker (Ferritin, LDH, d-dimers, CRP). All this information was routinely available at patients' admission and potential eligible individuals were identified by reviewing the new admissions' log of all COVID-19 units in the participating hospitals by study delegates or through direct referrals from COVID physicians. Those patients were then approached for the study and offered participation. Four study investigators were responsible for obtaining informed consent (IC) from the patients. Following signed IC, eligibility screening was taking place. If patients consented, were then formally screened for the presence of CD3+lymphopenia to determine full eligibility and enrollment. Eligible pts were randomized (2:1) to either receive COV-2-STs + SOC (Arm A) or SOC-alone (Arm B). Patient's randomization sequence was generated in RStudio using the Binomial distribution by an independent statistician and it remained concealed from the study investigators; for each codified entrance in the study the assigned treatment was revealed to investigators by telephone. Overall, based on the objective nature of the eligibility criteria and the small number of participating centers (n=2) we anticipate minimal, if any, recruitment bias.

Ethics oversight

The study was conducted in accordance with the Helsinki Declaration. Approval was obtained by jurisdictional ethics committees (National Ethics Committee and Institutional Review Board of George Papanikolaou and Hippokraton Hospitals) and our National Organization for Medicines (IS 052-21, 26/4/2021).

Note that full information on the approval of the study protocol must also be provided in the manuscript.

Field-specific reporting

Please select the one below that is the best fit for your research. If you are not sure, read the appropriate sections before making your selection.

Life sciences Behavioural & social sciences Ecological, evolutionary & environmental sciences

For a reference copy of the document with all sections, see nature.com/documents/nr-reporting-summary-flat.pdf

Life sciences study design

All studies must disclose on these points even when the disclosure is negative.

Sample size

The sample size was calculated based on the primary endpoint which was the recovery time. From the total sample size (656: 440/216) that was calculated based on a 2: 1 randomization ratio between the 2 arms, a recovery ratio equal to 1.35 (used in the remdesivir ACTT-1 trial study, including moderate to severe COVID-19 patients), $\alpha = 0.05$ and power 90%, a 13% (n=90) subset of the total sample size was deemed to be adequate for a phll trial, thus 60 and 30 people for the groups CoV-2-STs + SoC (Arm-A) and SoC (Arm-B), respectively planned for enrollment.

Data exclusions

90 patients met the inclusion criteria and were randomly assigned (2:1) to either Arm-A or Arm-B. Three patients withdrew consent and were excluded. One patient, initially allocated to CoV-2-STs-cohort, was intubated prior to receiving the cells so he was allocated to Arm B for the as-treated analysis. A total of 87/90 randomized patients were included in the intention-to-treat (Arm-A:58; Arm-B:29) and as-treated analysis

(Arm-A:57; Arm-B:30) (Figure 1F)

Replication	Findings were not replicated as this was a clinical trial.
Randomization	Patients were randomly assigned (2:1) to either CoV-2-STs+SoC or SoC-only by randomization with permuted blocks (size 3) to ensure balance between the 2 arms. Randomization sequence was generated in RStudio using the Binomial distribution by an independent statistician.
Blinding	This was an open label study. An open-label design was justified since patients allocated to CoV-2-ST-treated group needed to undergo HLA typing to receive a suitable cell product.

Reporting for specific materials, systems and methods

We require information from authors about some types of materials, experimental systems and methods used in many studies. Here, indicate whether each material, system or method listed is relevant to your study. If you are not sure if a list item applies to your research, read the appropriate section before selecting a response.

Materials & experimental systems

Methods

n/a	Involvement in the study	n/a	Involvement in the study
<input type="checkbox"/>	<input checked="" type="checkbox"/> Antibodies	<input checked="" type="checkbox"/>	<input type="checkbox"/> ChIP-seq
<input checked="" type="checkbox"/>	<input type="checkbox"/> Eukaryotic cell lines	<input type="checkbox"/>	<input checked="" type="checkbox"/> Flow cytometry
<input checked="" type="checkbox"/>	<input type="checkbox"/> Palaeontology and archaeology	<input checked="" type="checkbox"/>	<input type="checkbox"/> MRI-based neuroimaging
<input checked="" type="checkbox"/>	<input type="checkbox"/> Animals and other organisms		
<input type="checkbox"/>	<input checked="" type="checkbox"/> Clinical data		
<input checked="" type="checkbox"/>	<input type="checkbox"/> Dual use research of concern		

Antibodies

Antibodies used	<p>Marker, clone, cat number, supplier, dilution</p> <p>CD45 APC, 2D1, 340910, BD, 1:20</p> <p>CD3 FITC, UCHT1, 1F-514-T100, EXBIO, 1:5</p> <p>CD56 PE, C5.9, CYT-56PE, CYTOGNOS, 1:20</p> <p>CD4 PE-Cyanine5, RPA-T4, CYT-4C1, CYTOGNOS, 1:20</p> <p>CD3 APC, SK7, 345767, BD, 1:20</p> <p>CD8 PE, MEM-31, 1P-207-T100, EXBIO, 1:5</p> <p>CD45RA PE, MEM-56, 1P-223-T100, EXBIO, 1:5</p> <p>CD62L APC, LT-TD180, 1A-449-T100, EXBIO, 1:10</p> <p>Serum cytokines measurements multiplex cytokine assay (IL-6, IL-2, IL-10, TNFa, IFNg), C191051, AimPlex Biosciences</p>
Validation	<p>Commercial antibodies are validated by the manufacturer</p> <p>CD45 APC, 2D1, 340910, BD: CD45 is intended for in vitro diagnostic use in the identification of cells expressing the CD45 antigen, using a BD FACSTM brand flow cytometer. Regulatory Status: CE_IVD, reactivity: human, application: flow cytometry. Source: https://www.bdbiosciences.com/en-eu/products/reagents/flow-cytometry-reagents/clinical-diagnostics/single-color-antibodies-asr-ivd-ce-ivd/cd45-apc.340910</p> <p>CD3 FITC, UCHT1, 1F-514-T100, EXBIO: The antibody UCHT1 recognizes an extracellular epitope on CD3 antigen of the TCR/CD3 complex on mature human T cells. The UCHT1 antibody reacts with the epsilon chain of the CD3 complex. Reactivity: non-human primates, human. Application: Flow cytometry analysis (Quality Control method - each batch routinely tested). Source: https://www.exbio.cz/research-product/antibodies/cd-and-related-antigens/anti-hu-cd3-fitc-2?q=100+tests</p> <p>CD56 PE, C5.9, CYT-56PE, CYTOGNOS: CD56 is intended for in vitro diagnostic use in the identification of cells expressing the CD56 antigen by flow cytometry. Status: CE-IVD. Reactivity: human. Source: https://www.cytognos.com/products/cyt-56pe/</p> <p>CD4 PE-Cyanine5, RPA-T4, CYT-4C1, CYTOGNOS: Anti-human CD4-PE is a monoclonal antibody (mAb) labeled with R-phycoerythrin (PE) which has been designed to be used as a direct immunofluorescence reagent in order to identify cells that express the CD4 antigen by flow cytometry. It is to be used in bone marrow and/or peripheral blood. Status: CE-IVD. Source: https://www.cytognos.com/products/cyt-4pe1/</p> <p>CD3 APC, SK7, 345767, BD: CD3 is intended for in vitro diagnostic use in the identification of cells expressing the CD3 antigen, using a BD FACSTM brand flow cytometer. Regulatory Status: CE_IVD. Reactivity: human, application: flow cytometry. Source: https://www.bdbiosciences.com/en-eu/products/reagents/flow-cytometry-reagents/clinical-diagnostics/single-color-antibodies-asr-ivd-ce-ivd/cd3-apc.345767</p> <p>CD8 PE, MEM-31, 1P-207-T100, EXBIO: The antibody MEM-31 recognizes a conformationally-dependent extracellular epitope of CD8, a cell surface glycoprotein found on most cytotoxic T lymphocytes that mediates efficient cell-cell interactions within the immune system. CD8 is a disulfide-linked dimer and exists as a CD8 alpha/alpha homodimer or CD8 alpha/beta heterodimer (each monomer approx. 32-34 kDa). The antibody does not react with formaldehyde-fixed cells; negative in Western blotting application. Reactivity: human. Application: Flow cytometry analysis (Quality Control method - each batch routinely tested). Source: https://www.exbio.cz/research-product/antibodies/cd-and-related-antigens/anti-hu-cd8-pe?q=100+tests</p>

CD45RA PE, MEM-56, 1P-223-T100, EXBIO: The antibody MEM-56 reacts with an extracellular epitope of CD45RA, a 205-220 kDa single chain type I glycoprotein, variant of CD45 (CD45RA isoform). CD45RA is expressed on most of B lymphocytes, resting and native T lymphocytes, medullar thymocytes and monocytes. Reactivity: human. Application: Flow cytometry analysis (Quality Control method - each batch routinely tested). Source: <https://www.exbio.cz/research-product/antibodies/cd-and-related-antigens/anti-hu-cd45ra-pe>

CD62L APC, LT-TD180, 1A-449-T100, EXBIO: The antibody LT-TD180 reacts with an extracellular epitope of CD62L (L-selectin), a 74-95 kDa single chain type I glycoprotein expressed on most peripheral blood B lymphocytes, T lymphocytes, monocytes and granulocytes; it is also present on a subset of NK cells and certain hematopoietic malignant cells. Reactivity: human. Application: Flow cytometry analysis (Quality Control method - each batch routinely tested). Source: <https://www.exbio.cz/research-product/antibodies/cd-and-related-antigens/anti-hu-cd62l-apc?q=100+tests>

AimPlex Biosciences: Serum cytokines measurements multiplex cytokine assay. Reactivity: human. Application: Optimal antibody pairs and antigen standards for assaying Th1/Th2 5-Plex Panel 1. Source: <https://www.aimplexbio.com/humanth5p1>

Clinical data

Policy information about [clinical studies](#)

All manuscripts should comply with the ICMJE [guidelines for publication of clinical research](#) and a completed [CONSORT checklist](#) must be included with all submissions.

Clinical trial registration	EudraCT:2021-001022-22; NCT05447013
Study protocol	Study protocol is provided as a supplement to this manuscript.
Data collection	All data were collected at George Papanikolaou Hospital and Hippokrateion Hospital. Patients were enrolled between June 2nd 2021 and December 7th 2021 and were followed through January 5, 2022. Data recording was made in both paper and electronic Case Report Forms.
Outcomes	Major safety end-points were any acute toxicity associated with the cell therapy, the development of cytokine release syndrome (CRS) and the rates of adverse and severe adverse events (SAEs) in either arm. Secondary safety end-point was the development of graft-vs-host-disease (GvHD). The primary efficacy endpoint was the composite end point of time to recovery defined as the first day post-randomization (day-0) on which a patient scored ≤ 3 in the 8-category ordinal scale (OS, Table S9) and rate of recovery. A second primary end point was the in vivo expansion of CoV-2-STs. The key secondary outcome was day-60 survival. Other secondary outcomes included the time to PCR negatigation, time to lymphopenia recovery, hospitalization length, intubation/extubation incidence and in vivo persistence of donor CoV-2-STs. Primary and secondary outcomes were assessed through a review of the study CRFs. A complete description of the outcomes and their measurements is described in the manuscript and the study protocol.

Flow Cytometry

Plots

Confirm that:

- The axis labels state the marker and fluorochrome used (e.g. CD4-FITC).
- The axis scales are clearly visible. Include numbers along axes only for bottom left plot of group (a 'group' is an analysis of identical markers).
- All plots are contour plots with outliers or pseudocolor plots.
- A numerical value for number of cells or percentage (with statistics) is provided.

Methodology

Sample preparation	Immunophenotype of CoV-2-STs was determined after staining with antibodies that bind specifically to cell surface antigens, and subsequently washing the stained sample to remove excess antibody and debris. Absolute cell numbers were measured in peripheral blood by adding whole blood and fluorochrome-conjugated antibodies that bind specifically to cell surface antigens to truocount absolute counting tubes (BD Biosciences). Subsequently, lysing solution was added to the stained sample to lyse erythrocytes under gentle hypotonic conditions while preserving the leucocytes and the cells were analyzed. Cytokines were measured in the serum. Standard or serum samples were added to antibodies-beads and incubated. Subsequently, cells were washed and mixed with biotinylated antibodies. After incubation and washing, the samples were incubated with streptavidin-PE. The stained standards and samples were last washed and analyzed.
Instrument	Samples were acquired on a FACS Calibur device (Becton Dickinson, Switzerland).
Software	All analyses were performed with the CellQuest Pro6 software or FlowJo V10.
Cell population abundance	No cell sorting was performed in this work.

Gating strategy

Gating strategies are being presented in Figures S13-S15. In particular:

Gating strategy used to phenotypically characterize CoV-2-ST products (Figure S13): First CoV-2-STs were gated based on forward and side scatter to exclude debris. CD3 and CD8 expression or CD45RA and CD62L expression was then determined from this gated population. There was a very clear separation between the positive and negative populations. Gates were kept consistent between samples but were checked for each sample.

Gating strategy used to count the lymphocyte populations per μl of blood (Figure S14): The percentage of CD3, CD56 or CD4 expressing cells were identified by FSC vs SSC gating, followed by CD45 expression. The absolute number of CD3, CD56 and CD4 cells was counted based on the parallel measurement of absolute counting beads. There was a very clear separation between the positive and negative populations. Gates were kept consistent between samples but were checked for each sample.

Gating strategy used to measure serum cytokines (Figure S15): First, on an FSC vs SSC plot, one gate was created for the smaller beads and a 2nd gate was created for the larger beads. Four cytokines (IFN- γ , IL-2, IL-6, IL-10) were measured in the first gate and TNF- α in the second gate, based on manufacturer's instructions and standard curve created by standards provided in the KIT. Gates were kept consistent between samples but were checked for each sample.

Tick this box to confirm that a figure exemplifying the gating strategy is provided in the Supplementary Information.